THE EUROPEAN
PHYSICAL JOURNAL C

A two-tensor model with order-three

Bei Kang[1,a], Lu-Yao Wang[2,b], Ke Wu[2,c], Wei-Zhong Zhao[2,d]

[1] School of Mathematics and Statistics, North China University of Water Resources and Electric Power, Zhengzhou 450046, Henan, China
[2] School of Mathematical Sciences, Capital Normal University, Beijing 100048, China

Abstract We construct a two-tensor model with order-3 and present its W-representation. Moreover we derive the compact expressions of correlators from the W-representation and analyze the free energy in large N limit. In addition, we establish the correspondence between two colored Dyck walks in the Fredkin spin chain and tree operators in the ring. Based on the classification Dyck walks, we give the number of tree operators with the given level. Furthermore, we show the entanglement scaling of Fredkin spin chain beyond logarithmic scaling in the ordinary critical systems from the viewpoint of tensor model.

1 Introduction

Matrix models can be associated with discretized random surfaces and $2D$ quantum gravity [1]. For the perturbative series of matrix models, one can rewrite them as a series in $1/N$ indexed by the genus, where N is the size of the matrix. At leading order, the ordinary topological expansion of matrix models dominated by planar graphs. This limit has been widely studied and has led to a plethora of results, in particular their continuum limit and integrability. As the generalizations of matrix models from matrices to tensors, tensor models were originally introduced to describe the higher dimensional quantum gravity [2–4]. The $1/N$ expansion for colored tensor models was identified in [5–8], where colored tensors are tensors with no further tensorial symmetry assumed (and an additional flavor index called color). It was shown that tensor models admit a specific kind of large N limit, the so-called melonic limit [5–10]. In this limit, the dominant melonic graphs are built recursively by two-point

insertions on an initial two-point diagram. Much progress has been made in recent years on colored tensor models, which has stimulated other fields. For instance, the existence of $1/N$ expansion for tensor has triggered a series of investigations on the renormalization group analysis of the quantum field theoretic counterpart of tensor models, i.e. tensor field theory [11–14]. Importantly, it was shown that in specific instances, these quantum field models are asymptotically free [15–17]. Concerning the large N expansion of tensor models, it turns out that coloration was not a prerequisite for the discovery of such an expansion: Gurau [18] proposed a new approach to the $1/N$ expansion adapted to symmetric (and antisymmetric) tensors. It was proved that a tensor model with two symmetric tensors and interactions the complete graph admits a $1/N$ expansion. Moreover, for the symmetric traceless and the antisymmetric tensor models in rank-3 with tetrahedral interaction, it was found that they admit a $1/N$ expansion [19]. Universally, at leading order, all these models are dominated by melonic diagrams.

Tensor models have found also intriguing connections with gauge-string duality. By applying permutation TFT methods, Ben Geloun and Ramgoolam [20] counted gauge invariants for tensor models and obtained some formulae for correlators of the tensor model invariants. Furthermore, they showed that the counting of observables and correlators for a 3-index tensor model are organized by the structure of a family of permutation centralizer algebras [21]. Collective field theory provides a systematic construction of the dynamics of invariant observables of the theory. It has been applied in the analysis of tensor models, such as the large N dynamics of the boson tensor model quantum mechanics [22] and holographic duals of tensor models [23]. Rainbow tensor model which has gauge symmetry $U(N_1) \bigotimes \cdots \bigotimes U(N_r)$ is a direct generalization of rectangular complex matrix model with rectangular matrix substituted by a complex-valued tensor of rank-r [24–27]. In rainbow tensor model, all the planar diagrams are automatically melonic. Once again, just as

[a] e-mail: kangbei@ncwu.edu.cn

[b] e-mail: wangly100@outlook.com

[c] e-mail: wuke@cnu.edu.cn

[d] e-mail: zhaowz@cnu.edu.cn (corresponding author)

any tensor models with no symmetry assumed between the tensor indices, melonic graphs are dominant in the large N limit of rainbow tensor models. The simplest rainbow tensor model is the Aristotelian RGB (red-green-blue) model with a single complex tensor of rank-3 and the RGB symmetry $U(N_1) \bigotimes U(N_2) \bigotimes U(N_3)$. With the example of the Aristotelian RGB model, Itoyama et al. [24] introduced a few methods which allow one to connect calculations in the tensor models to those in the matrix models. Furthermore, it was found that there are some new factorization formulas and sum rules for the Gaussian correlators in the Hermitian and complex matrix theories, square and rectangular.

W-representation of matrix model was proposed by Morozov and Shakirov for the realization of partition function by acting on elementary functions with exponents of the given *W*-operator [28]. The superintegrable matrix models can be analyzed from the viewpoint of *W*-representations [29–34]. The progress has been made on *W*-representations of tensor models. As was expected, the Gaussian tensor model with Gaussian action can be realized by the *W*-representation [35]. Moreover, from its character expansion with respect to the Schur functions, it turned out that this model is superintegrable. The *W*-representation of rainbow tensor model has been investigated [36,37]. In this paper, we will make a step towards the *W*-representation of a two-tensor model with order-3,[1,2] and analyze the correlators and free energy.

This paper is organized as follows. In Sect. 2, we give the keystone operators and construct a graded ring with tree and loop operators. The kernel and cokernel of the cut-and-join structure in the graded ring are investigated. Then we establish the correspondence between two colored Dyck walks in the Fredkin spin chain and tree operators. Based on the classification Dyck walks, we present the number of tree operators with the given level. Moreover for the entanglement entropy of the Fredkin spin chain, we show the entanglement scaling beyond logarithmic scaling in the ordinary critical systems from the viewpoint of tensor model. In Sect. 3, we construct a two-tensor model with order-3 and present its *W*-representation. In terms of the *W*-representation, we derive the compact expression of correlators. Using the collective field, we also calculate the correlators. Furthermore we discuss the free energy and its large N limit. We end this paper with the conclusions in Sect. 4. We list some results of cut operation Δ and kernel in the Appendix.

---

[1] Here we use "order" instead of "rank" since the rank of a tensor is defined by the minimal number of tensors of order 1 required to express a tensor as a sum of such tensors.

[2] The two-tensor model that we deal with can be seen as the two-tensor extension associated with "uncolored" tensor model defined in [38].

2 The graded ring of gauge-invariant operators

2.1 Gauge invariants and cut-join operators

Let us consider the tensor fields $A_i^{j_1,j_2}$ and $B_i^{j_1,j_2}$ with order-3 which transform in the fundamental of $G = U(N_1) \times U(N_2) \times U(N_3)$, where $i = 1, \ldots, N_1$, $j_1 = 1, \ldots, N_2$ and $j_2 = 1, \ldots, N_3$. We denote V_k the vector space carrying a copy of the fundamental representation of $U(N_k)$. The fields transforming in the fundamental of $G = U(N_1) \times U(N_2) \times U(N_3)$ belong to $V_1 \times V_2 \times V_3$. To build gauge invariants, we introduce the conjugate tensor fields that transform in the anti-fundamental, denoted $\bar{A}_{j_1,j_2}^i$ and $\bar{B}_{j_1,j_2}^i$. Then the gauge invariants with level-$(n+m)$ are given by contracting corresponding upper and lower indices, denoted formally as [20,22]

$$
\begin{aligned}
\mathcal{T}_{\check{\sigma}}^{(n,m)} &\equiv \mathcal{T}_{(\sigma_1,\sigma_2,\sigma_3)}^{(n,m)} = \mathcal{A}_I^{J_1,J_2} \cdot (\sigma_1, \sigma_2, \sigma_3) \cdot \bar{\mathcal{A}}_{J_1,J_2}^I \\
&= \mathcal{A}_I^{J_1,J_2} \bar{\mathcal{A}}_{\sigma_2(J_1),\sigma_3(J_2)}^{\sigma_1(I)},
\end{aligned} \tag{2.1}
$$

where n and m are non-negative integers satisfying $n+m \geqslant 1$, and the action $\check{\sigma} \equiv (\sigma_1, \sigma_2, \sigma_3) \in S_{n+m} \times S_{n+m} \times H_{n,m}$ acts independently on three indices of $\bar{\mathcal{A}}_{J_1,J_2}^I$, where S_{n+m} is the permutation group, and $H_{n,m} \equiv S_n \times S_m$ is a subgroup of S_{n+m}. The sleek notation uses the capital Roman letters I, J_1, J_2 to collect all of the little Roman letter indices, for example I stands for $i^{(1)}, i^{(2)}, \ldots, i^{(n+m)}$. Repeated indices are summed over in (2.1) and the following text. $\mathcal{A}_I^{J_1,J_2}$, $\bar{\mathcal{A}}_{J_1,J_2}^I$ and $\bar{\mathcal{A}}_{\sigma_2(J_1),\sigma_3(J_2)}^{\sigma_1(I)}$ are given by

$$
\begin{aligned}
\mathcal{A}_I^{J_1,J_2} &= A_{i^{(1)}}^{j_1^{(1)},j_2^{(1)}} \cdots A_{i^{(n)}}^{j_1^{(n)},j_2^{(n)}} B_{i^{(n+1)}}^{j_1^{(n+1)},j_2^{(n+1)}} \\
&\quad \cdots B_{i^{(n+m)}}^{j_1^{(n+m)},j_2^{(n+m)}}, \\
\bar{\mathcal{A}}_{J_1,J_2}^I &= \bar{A}_{j_1^{(1)},j_2^{(1)}}^{i^{(1)}} \cdots \bar{A}_{j_1^{(n)},j_2^{(n)}}^{i^{(n)}} \bar{B}_{j_1^{(n+1)},j_2^{(n+1)}}^{i^{(n+1)}} \\
&\quad \cdots \bar{B}_{j_1^{(n+m)},j_2^{(n+m)}}^{i^{(n+m)}},
\end{aligned}
$$

$$
\begin{aligned}
\bar{\mathcal{A}}_{\sigma_2(J_1),\sigma_3(J_2)}^{\sigma_1(I)} &= (\sigma_1, \sigma_2, \sigma_3) \cdot \bar{\mathcal{A}}_{J_1,J_2}^I \\
&= \bar{A}_{j_1^{\sigma_2(1)},j_2^{\sigma_3(1)}}^{i^{\sigma_1(1)}} \cdots \bar{A}_{j_1^{\sigma_2(n)},j_2^{\sigma_3(n)}}^{i^{\sigma_1(n)}} \\
&\quad \bar{B}_{j_1^{\sigma_2(n+1)},j_2^{\sigma_3(n+1)}}^{i^{\sigma_1(n+1)}} \cdots \bar{B}_{j_1^{\sigma_2(n+m)},j_2^{\sigma_3(n+m)}}^{i^{\sigma_1(n+m)}}.
\end{aligned} \tag{2.2}
$$

Here we denote $\sigma_1(I) = (i^{\sigma_1(1)}, \ldots, i^{\sigma_1(n+m)})$ and similarly for $\sigma_2(J_1)$ and $\sigma_3(J_2)$. Note that $\mathcal{T}_{\check{\sigma}}^{(0,m)}$ and $\mathcal{T}_{\check{\sigma}}^{(n,0)}$ are exactly the gauge invariants in Aristotelian RGB model [24]. Since $\sigma_3 \in S_n \times S_m$, we actually focus on a subset of gauge invariants with all possible contractions where

(i) for $A_i^{j_1,j_2}$ and $\bar{B}_{j_1',j_2'}^{i'}$ (or $B_{i'}^{j_1',j_2'}$ and $\bar{A}_{j_1,j_2}^i$), we do not contract the indices j_2 and j_2';

(ii) no contractions are possible for $A_i^{j_1,j_2}$ and $B_{i'}^{j_1',j_2'}$ (and $\bar{A}_{j_1,j_2}^i$ and $\bar{B}_{j_1',j_2'}^{i'}$).

As done in [24], let us take the following six operators as the so-called keystone operators

$$
\begin{aligned}
\mathcal{T}_{((12),id,id)}^{(2,0)} &= A_{i^{(1)}}^{j_1^{(1)},j_2^{(1)}} \bar{A}_{j_1^{(1)},j_2^{(1)}}^{i^{(2)}} A_{i^{(2)}}^{j_1^{(2)},j_2^{(2)}} \bar{A}_{j_1^{(2)},j_2^{(2)}}^{i^{(1)}}, \\
\mathcal{T}_{(id,(12),id)}^{(2,0)} &= A_{i^{(1)}}^{j_1^{(1)},j_2^{(1)}} \bar{A}_{j_1^{(2)},j_2^{(1)}}^{i^{(1)}} A_{i^{(2)}}^{j_1^{(2)},j_2^{(2)}} \bar{A}_{j_1^{(1)},j_2^{(2)}}^{i^{(2)}}, \\
\mathcal{T}_{((12),id,id)}^{(0,2)} &= B_{i^{(1)}}^{j_1^{(1)},j_2^{(1)}} \bar{B}_{j_1^{(1)},j_2^{(1)}}^{i^{(2)}} B_{i^{(2)}}^{j_1^{(2)},j_2^{(2)}} \bar{B}_{j_1^{(2)},j_2^{(2)}}^{i^{(1)}}, \\
\mathcal{T}_{(id,(12),id)}^{(0,2)} &= B_{i^{(1)}}^{j_1^{(1)},j_2^{(1)}} \bar{B}_{j_1^{(2)},j_2^{(1)}}^{i^{(1)}} B_{i^{(2)}}^{j_1^{(2)},j_2^{(2)}} \bar{B}_{j_1^{(1)},j_2^{(2)}}^{i^{(2)}}, \\
\mathcal{T}_{((12),id,id)}^{(1,1)} &= A_{i^{(1)}}^{j_1^{(1)},j_2^{(1)}} \bar{A}_{j_1^{(1)},j_2^{(1)}}^{i^{(2)}} B_{i^{(2)}}^{j_1^{(2)},j_2^{(2)}} \bar{B}_{j_1^{(2)},j_2^{(2)}}^{i^{(1)}}, \\
\mathcal{T}_{(id,(12),id)}^{(1,1)} &= A_{i^{(1)}}^{j_1^{(1)},j_2^{(1)}} \bar{A}_{j_1^{(2)},j_2^{(1)}}^{i^{(1)}} B_{i^{(2)}}^{j_1^{(2)},j_2^{(2)}} \bar{B}_{j_1^{(1)},j_2^{(2)}}^{i^{(2)}}. \quad (2.3)
\end{aligned}
$$

Since $\mathcal{T}_{\check{\sigma}}^{(n,m)}$ with the different σ_1, σ_2 and σ_3 may give the same gauge invariant, we need not discuss the case of a non id permutation on the third slot.

For the gauge-invariant operator $\mathcal{T}_{\check{\alpha}}^{(a,b)}$, $\check{\alpha}$ is a permutation about $a+b$ elements, and $a+b$ is the level of $\mathcal{T}_{\check{\alpha}}^{(a,b)}$, we denote level($\check{\alpha}$) = $a+b$. Let us introduce the cut and join operations on the gauge-invariant operator $\mathcal{T}_{\check{\alpha}}^{(a,b)}$ as follows. The actions of the cut operations on the gauge-invariant operator $\mathcal{T}_{\check{\alpha}}^{(a,b)}$ are

$$
\begin{aligned}
\Delta \mathcal{T}_{\check{\alpha}}^{(a,b)} &= \sum_{i=1}^{N_1} \sum_{j_1=1}^{N_2} \sum_{j_2=1}^{N_3} \frac{\partial^2 \mathcal{T}_{\check{\alpha}}^{(a,b)}}{\partial A_i^{j_1,j_2} \partial \bar{A}_{j_1,j_2}^i} \\
&= \sum_{k=1}^{3} \sum_{\substack{a_1+\cdots+a_k+1=a \\ b_1+\cdots+b_k=b \\ as\,ps_1 \leq a_2 \leq \cdots \leq a_k}} \sum_{\check{\beta}_1,\ldots,\check{\beta}_k} \Delta_{\check{\alpha},\check{\beta}_1,\ldots,\check{\beta}_k}^{(a,b),(a_1,b_1),\ldots,(a_k,b_k)} \mathcal{T}_{\check{\beta}_1}^{(a_1,b_1)} \\
&\qquad \cdots \mathcal{T}_{\check{\beta}_k}^{(a_k,b_k)}, \quad a+b \geqslant 2, \\
\tilde{\Delta} \mathcal{T}_{\check{\alpha}}^{(a,b)} &= \sum_{i=1}^{N_1} \sum_{j_1=1}^{N_2} \sum_{j_2=1}^{N_3} \frac{\partial^2 \mathcal{T}_{\check{\alpha}}^{(a,b)}}{\partial B_i^{j_1,j_2} \partial \bar{B}_{j_1,j_2}^i} \\
&= \sum_{k=1}^{3} \sum_{\substack{a_1+\cdots+a_k=a \\ b_1+\cdots+b_k+1=b \\ bs\,ps_1 \leq b_2 \leq \cdots \leq b_k}} \sum_{\check{\gamma}_1,\ldots,\check{\gamma}_k} \tilde{\Delta}_{\check{\alpha},\check{\gamma}_1,\ldots,\check{\gamma}_k}^{(a,b),(a_1,b_1),\ldots,(a_k,b_k)} \mathcal{T}_{\check{\gamma}_1}^{(a_1,b_1)} \\
&\qquad \cdots \mathcal{T}_{\check{\gamma}_k}^{(a_k,b_k)}, \quad a+b \geqslant 2, \quad (2.4)
\end{aligned}
$$

where level($\check{\beta}_i$) = $a_i + b_i$ ($i = 1,\ldots,k$), level($\check{\gamma}_j$) = $a_j + b_j$ ($j=1,\ldots,k$), $\Delta_{\check{\alpha},\check{\beta}_1,\ldots,\check{\beta}_k}^{(a,b),(a_1,b_1),\ldots,(a_k,b_k)}$ and $\tilde{\Delta}_{\check{\alpha},\check{\gamma}_1,\ldots,\check{\gamma}_k}^{(a,b),(a_1,b_1),\ldots,(a_k,b_k)}$ are polynomials in N_i with integer coefficients (see examples in (A.1)).

The actions of the join operations on the gauge-invariant operator $\mathcal{T}_{\check{\alpha}}^{(a,b)}$ and $\mathcal{T}_{\check{\beta}}^{(c,d)}$ are

$$
\begin{aligned}
\left\{ \mathcal{T}_{\check{\alpha}}^{(a,b)}, \mathcal{T}_{\check{\beta}}^{(c,d)} \right\}_A &= \sum_{i=1}^{N_1} \sum_{j_1=1}^{N_2} \sum_{j_2=1}^{N_3} \frac{\partial \mathcal{T}_{\check{\alpha}}^{(a,b)}}{\partial A_i^{j_1,j_2}} \frac{\partial \mathcal{T}_{\check{\beta}}^{(c,d)}}{\partial \bar{A}_{j_1,j_2}^i} \\
&= \sum_{\check{\gamma} \mid \text{level}(\check{\gamma})=a+b+c+d-1} \Lambda_{\check{\alpha},\check{\beta},\check{\gamma}}^{(a,b),(c,d),(a+c-1,b+d)} \\
&\quad \times \mathcal{T}_{\check{\gamma}}^{(a+c-1,b+d)}, \\
\left\{ \mathcal{T}_{\check{\alpha}}^{(a,b)}, \mathcal{T}_{\check{\beta}}^{(c,d)} \right\}_B &= \sum_{i=1}^{N_1} \sum_{j_1=1}^{N_2} \sum_{j_2=1}^{N_3} \frac{\partial \mathcal{T}_{\check{\alpha}}^{(a,b)}}{\partial B_i^{j_1,j_2}} \frac{\partial \mathcal{T}_{\check{\beta}}^{(c,d)}}{\partial \bar{B}_{j_1,j_2}^i} \\
&= \sum_{\check{\sigma} \mid \text{level}(\check{\sigma})=a+b+c+d-1} \tilde{\Lambda}_{\check{\alpha},\check{\beta},\check{\sigma}}^{(a,b),(c,d),(a+c-1,b+d)} \\
&\quad \times \mathcal{T}_{\check{\sigma}}^{(a+c-1,b+d)}, \quad (2.5)
\end{aligned}
$$

where $\Lambda_{\check{\alpha},\check{\beta},\check{\gamma}}^{(a,b),(c,d),(a+c-1,b+d)}$ and $\tilde{\Lambda}_{\check{\alpha},\check{\beta},\check{\sigma}}^{(a,b),(c,d),(a+c-1,b+d)}$ are integer coefficients (see examples in Table 1). Here for clarity of classifying and generating structure of the gauge invariants, the cut and join operations (2.4) and (2.5) involve only A and $\bar{A}$, or B and $\bar{B}$, and do not contain A and $\bar{B}$, or B and $\bar{A}$.

To draw the graph associated to the gauge invariants, we represent every tensor field by a white vertex and its conjugation by a black vertex. We promote the position of an index to a color: i has color 1, j_1 has color 2 and j_2 has color 3. Lines inherit the color of the index, and always connect a black and a white vertex. The direction of arrow depends on the choice of covariant and contravariant indices, which is from the tensor field to its conjugate. The gauge invariants $\mathcal{T}_{((12\cdots m),id,id)}^{(n,m)}$ and $\mathcal{T}_{(id,(12\cdots m),id)}^{(n,m)}$ with given length-$(n+m)$ can be depicted as $(n+m)$ indexed circles "**I**" and "**II**", respectively (see Fig. 1).

By means of the keystone operators (2.3), we may construct a graded ring $\mathcal{S}$ with tree and loop operators, where $\mathcal{S}$ is generated by the keystone operators with addition, multiplication, cut and join operations. $\mathcal{S} = \sum_{l=1}^{\infty} \mathcal{S}_l$, where $\mathcal{S}_l$ consists of the gauge invariants with level l. Note that for the tree and loop operators, they have the similar construction rules with the Aristotelian tensor model. We use the black dotted lines to represent the Feynman propagators.

The tree operators made from (2.3) alone are constructed by merging two vertices in two concentric circles (propagators) of the same color (see Fig. 2a and b). When tree operators involve chains with both circles **I** and **II**, they can be constructed by merging two vertices of two circles (propagators) of different index (see Fig. 2c and d).

The loop operators made from (2.3) alone are constructed by merging two vertices inside circles (propagators) (see Fig. 3a and b). When loop operators involve both circles
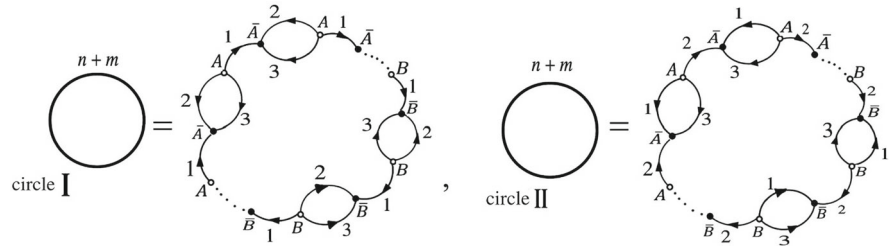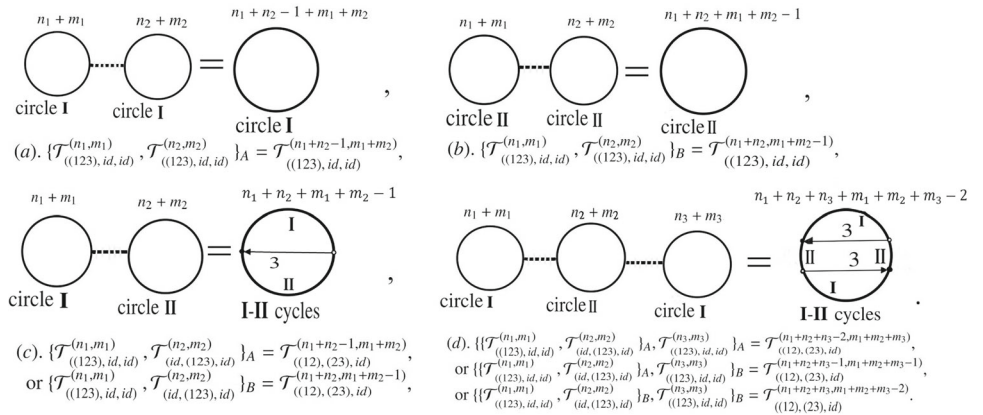
Fig. 1 Circles **I** and **II**

Fig. 2 Tree operators

(a). $\{\mathcal{T}^{(n_1,m_1)}_{((123),\,id,\,id)},\,\mathcal{T}^{(n_2,m_2)}_{((123),\,id,\,id)}\}_A = \mathcal{T}^{(n_1+n_2-1,m_1+m_2)}_{((123),\,id,\,id)}$,

(b). $\{\mathcal{T}^{(n_1,m_1)}_{((123),\,id,\,id)},\,\mathcal{T}^{(n_2,m_2)}_{((123),\,id,\,id)}\}_B = \mathcal{T}^{(n_1+n_2,m_1+m_2-1)}_{((123),\,id,\,id)}$,

(c). $\{\mathcal{T}^{(n_1,m_1)}_{((123),\,id,\,id)},\,\mathcal{T}^{(n_2,m_2)}_{(id,\,(123),\,id)}\}_A = \mathcal{T}^{(n_1+n_2-1,m_1+m_2)}_{((12),\,(23),\,id)}$,

or $\{\mathcal{T}^{(n_1,m_1)}_{((123),\,id,\,id)},\,\mathcal{T}^{(n_2,m_2)}_{(id,\,(123),\,id)}\}_B = \mathcal{T}^{(n_1+n_2,m_1+m_2-1)}_{((12),\,(23),\,id)}$,

(d). $\{\{\mathcal{T}^{(n_1,m_1)}_{((123),\,id,\,id)},\,\mathcal{T}^{(n_2,m_2)}_{(id,\,(123),\,id)}\}_A,\,\mathcal{T}^{(n_3,m_3)}_{((123),\,id,\,id)}\}_A = \mathcal{T}^{(n_1+n_2+n_3-2,m_1+m_2+m_3)}_{((12),\,(23),\,id)}$,

or $\{\{\mathcal{T}^{(n_1,m_1)}_{((123),\,id,\,id)},\,\mathcal{T}^{(n_2,m_2)}_{(id,\,(123),\,id)}\}_A,\,\mathcal{T}^{(n_3,m_3)}_{((123),\,id,\,id)}\}_B = \mathcal{T}^{(n_1+n_2+n_3-1,m_1+m_2+m_3-1)}_{((12),\,(23),\,id)}$,

or $\{\{\mathcal{T}^{(n_1,m_1)}_{((123),\,id,\,id)},\,\mathcal{T}^{(n_2,m_2)}_{(id,\,(123),\,id)}\}_B,\,\mathcal{T}^{(n_3,m_3)}_{((123),\,id,\,id)}\}_B = \mathcal{T}^{(n_1+n_2+n_3,m_1+m_2+m_3-2)}_{((12),\,(23),\,id)}$.

I and **II**, they are either the **I**–**II** cycles with the intersecting shortcuts of color 3 or several such **I**–**II** cycles with the shortcuts connected by lines of color 3 (see Fig. 3c and d), which are constructed by merging two vertices in two circles (propagators) of two different indexes.

Note that **I**–**II** cycles form a circle with length-$(n + m)$ divided into segments through the arrow line of color 3 (see Figs. 2c, d and 3c, d). The segments can be drawn as lines labeled "**I**" or "**II**" with length-$(n' + m')$, and $n' \leq n$, $m' \leq m$ (see Fig. 4).

As done in Ref. [24], if we consider merging two vertices in two segments **I** and **II**, then it leads to emerging of two new inter-propagator vertices connected by a arrow line of color 3. Pictorially:

2.2 Counting gauge-invariant operators

Let us focus on the gauge invariants $\mathcal{T}^{(n,m)}_{\vec{\sigma}}$ with fixed positive integers n, m in the graded ring $\mathcal{S}$. $H_{n,m}$ acts on the left on $\mathcal{A}^{J_1,J_2}_I$ by simply swapping the tensors A among themselves and the tensors B among themselves. Similarly, $H_{n,m}$ acts on the right on $\bar{\mathcal{A}}^I_{J_1,J_2}$ by swapping the tensors $\bar{A}$ among themselves and the tensors $\bar{B}$ among themselves. Let h_1, $h_2 \in H_{n,m}$, thus

$$
\begin{aligned}
\mathcal{A}^{J_1,J_2}_I &\cdot (\sigma_1,\sigma_2,\sigma_3) \cdot \bar{\mathcal{A}}^I_{J_1,J_2} \\
&= (\mathcal{A}^{J_1,J_2}_I \cdot h_1) \cdot (\sigma_1,\sigma_2,\sigma_3) \cdot (h_2 \cdot \bar{\mathcal{A}}^I_{J_1,J_2}) \\
&= \mathcal{T}^{(n,m)}_{(h_1\sigma_1 h_2,\,h_1\sigma_2 h_2,\,h_1\sigma_3 h_2)}.
\end{aligned}
\tag{2.7}
$$

$$
(\mathrm{Tr}\,\frac{\partial}{\partial\bar{A}}\frac{\partial}{\partial A})[\cdots A^{j_1^{(s)},j_2^{(s)}}_{i^{(s)}}\,\bar{A}^{i^{(s)}}_{j_1^{(s+1)},j_2^{(s)}}\hat{O}^{j_1^{(s+1)}}_{j_1^{(r)}}][\hat{O}'^{i^{(q)}}_{i^{(k)}}A^{j_1^{(q)},j_2^{(q)}}_{i^{(q)}}\bar{A}^{i^{(l)}}_{j_1^{(q)},j_2^{(q)}}\cdots] = [\cdots A^{j_1^{(s)},j_2^{(s)}}_{i^{(s)}}\hat{O}^{j_1^{(s+1)}}_{j_1^{(r)}}][\hat{O}'^{i^{(q)}}_{i^{(k)}}\bar{A}^{i^{(l)}}_{j_1^{(q)},j_2^{(q)}}\cdots]
\tag{2.6}
$$

Fig. 3 Loop operators

$(a). \Delta\mathcal{T}^{(n_1+n_2,m_1+m_2)}_{((123),id,id)} = \mathcal{T}^{(n_1,m_1)}_{((123),id,id)} \mathcal{T}^{(n_2-1,m_2)}_{((123),id,id)},$

$(b). \tilde{\Delta}\mathcal{T}^{(n_1+n_2,m_1+m_2)}_{((123),id,id)} = \mathcal{T}^{(n_1,m_1)}_{((123),id,id)} \mathcal{T}^{(n_2,m_2-1)}_{((123),id,id)},$

$(c). \Delta(\{\mathcal{T}^{(n_1,m_1)}_{((123),id,id)}, \mathcal{T}^{(n_2,m_2)}_{(id,(123),id)}\}_A) = \Delta\mathcal{T}^{(n_1+n_2-1,m_1+m_2)}_{((12),(23),id)},$
$\text{or } \tilde{\Delta}(\{\mathcal{T}^{(n_1,m_1)}_{((123),id,id)}, \mathcal{T}^{(n_2,m_2)}_{(id,(123),id)}\}_A) = \Delta\mathcal{T}^{(n_1+n_2,m_1+m_2-1)}_{((12),(23),id)},$

$(d). \Delta(\{\Delta(\{\mathcal{T}^{(n_1,m_1)}_{((123),id,id)}, \mathcal{T}^{(n_2,m_2)}_{(id,(123),id)}\}_A), \mathcal{T}^{(n_3,m_3)}_{((123),id,id)}\}_A),$
$\text{or } \tilde{\Delta}(\{\tilde{\Delta}(\{\mathcal{T}^{(n_1,m_1)}_{((123),id,id)}, \mathcal{T}^{(n_2,m_2)}_{(id,(123),id)}\}_B), \mathcal{T}^{(n_3,m_3)}_{((123),id,id)}\}_B).$
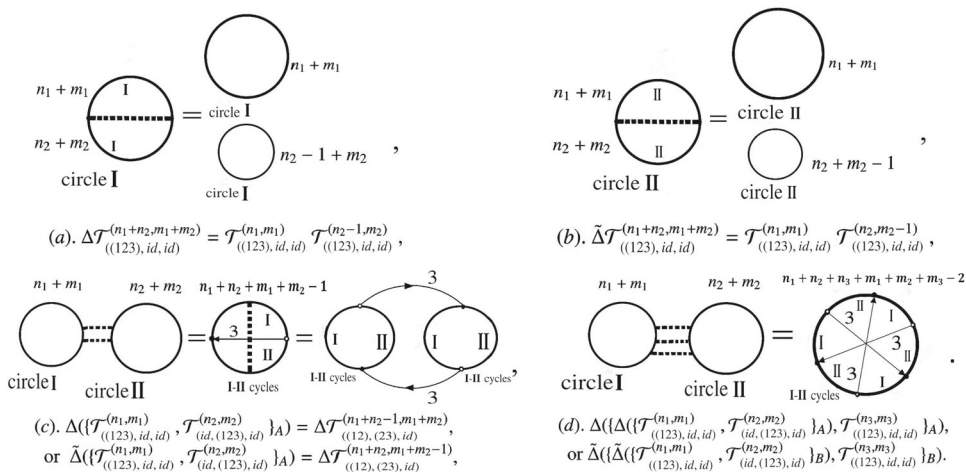
We see that $\mathcal{T}^{(n,m)}_{\vec{\sigma}}$ and $\mathcal{T}^{(n,m)}_{(h_1\sigma_1 h_2,\, h_1\sigma_2 h_2,\, h_1\sigma_3 h_2)}$ are indeed the same gauge-invariant operator. It implies that σ_i, $i = 1, 2, 3$, in $\mathcal{T}^{(n,m)}_{\vec{\sigma}}$ are characterized by the double coset $H_{n,m} \backslash S_{n+m} \times S_{n+m} \times H_{n,m}/H_{n,m}$ [20,21].

For a permutation p in S_l, the size of conjugacy class $|T_p|$ is given by $|T_p| = \frac{l!}{Sym_l(p)}$, where $Sym_l(p) = \prod_{i=1}^{N}(i^{p_i})(p_i!)$ is the number of elements of S_l commuting with any permutation in the conjugacy class T_p, and p_i gives the number of cycles of size i in p. Let us take $h_2 = gk$, where $g \in S_n$, $k \in S_m$. By Burnside's Lemma, the number of elements in this double coset is

$$|H_{n,m} \backslash S_{n+m} \times S_{n+m} \times H_{n,m}/H_{n,m}|$$
$$= \frac{1}{|H_{n,m}|^2} \sum_{h_1,h_2,\sigma_3 \in H_{n,m}} \sum_{\sigma_1,\sigma_2 \in S_{n+m}} \delta(h_1\sigma_1 h_2\sigma_1^{-1})$$
$$\times \delta(h_1\sigma_2 h_2\sigma_2^{-1})\delta(h_1\sigma_3 h_2\sigma_3^{-1})$$
$$= \frac{1}{|H_{n,m}|^2} \sum_{h_2 \in H_{n,m}} \frac{n!}{Sym_n(g)} \cdot \frac{m!}{Sym_m(k)}$$
$$\cdot (Sym_{n+m}(h_2))^2 \cdot Sym_n(g) \cdot Sym_m(k)$$
$$= \frac{1}{|H_{n,m}|} \sum_{h \in H_{n,m}} (Sym_{n+m}(h))^2. \qquad (2.8)$$

For the given h_2 and h_1 in T_{h_2} in the second line of (2.8), $\delta(h_1\sigma_i h_2\sigma_i^{-1})$, $i = 1, 2$ constraints σ_i to be the permutations in S_{n+m} commuting with any permutation in T_{h_2}, which is exactly $Sym_{n+m}(h_2)$. $\delta(h_1\sigma_3 h_2\sigma_3^{-1})$ limits the sum over σ_3 to select only the permutations which commute with any element of the conjugacy class of h_2 seen as an element of $S_n \times S_m$. This yields $Sym_n(g)Sym_m(k)$.

For example, when $n = m = 1$, $H_{1,1}$ only contains the identity mapping $id = (1)(2)$, and $Sym_{1+1}(id) = Sym_2(id) = 1^2 \cdot 2! = 2$, then

$$|H_{1,1} \backslash S_2 \times S_2 \times H_{1,1}/H_{1,1}| = (Sym_{1+1}(id))^2 = 2^2 = 4. \qquad (2.9)$$
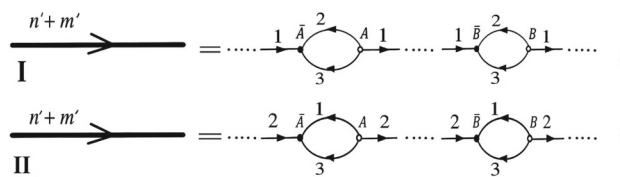
Fig. 4 Propagators

Table 1 Examples with different n and m

n	m	$|H_{n,m}|$	$|H_{n,m}\backslash S_{n+m} \times S_{n+m} \times H_{n,m}/H_{n,m}|$
1	3	6	107
1	4	24	660
2	2	4	168
2	3	12	1276
3	3	36	16084

For the case of $n = 1$ and $m = 2$, $H_{1,2} = \{id = (1)(2)(3), (1)(23)\}$ in (2.8), then $Sym_{1+2}(id) = Sym_3(id) = 1^3 \cdot 3! = 6$, $Sym_{1+2}((1)(23)) = Sym_3((1)(23)) = 1^1 \cdot 2^1 \cdot 1! \cdot 1! = 2$, we have

$$|H_{1,2} \backslash S_3 \times S_3 \times H_{1,2}/H_{1,2}|$$
$$= \frac{1}{2}((Sym_{1+2}(id))^2 + (Sym_{1+2}((1)(23)))^2)$$
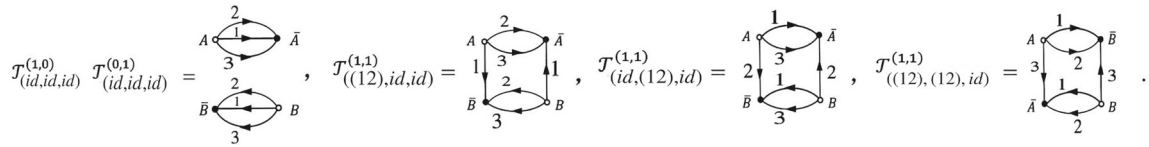$$= \frac{1}{2}(6^2 + 2^2) = 20. \qquad (2.10)$$

Let us list more examples in Table 1.

We draw the operators of the cases (2.9) and (2.10) in Figs. 5 and 6, respectively.

Thus the number of independent operators at each level-l is

$$\sharp_l = \sum_{n=1}^{l-1} \frac{1}{|H_{n,l-n}|} \sum_{h \in H_{n,l-n}} (Sym_l(h))^2 + 2\sum_{p \vdash l} Sym_l(p), \qquad (2.11)$$

Fig. 5 Four operators in the case of $n = 1$ and $m = 1$ in (2.9). White dots correspond to tensor fields $A_i^{j_1,j_2}$ and $B_i^{j_1,j_2}$, black dots to $\bar{A}^i_{j_1,j_2}$ and $\bar{B}^i_{j_1,j_2}$; lines of colors 1, 2 and 3 represent the contracting i, j_1 and j_2 indices, respectively
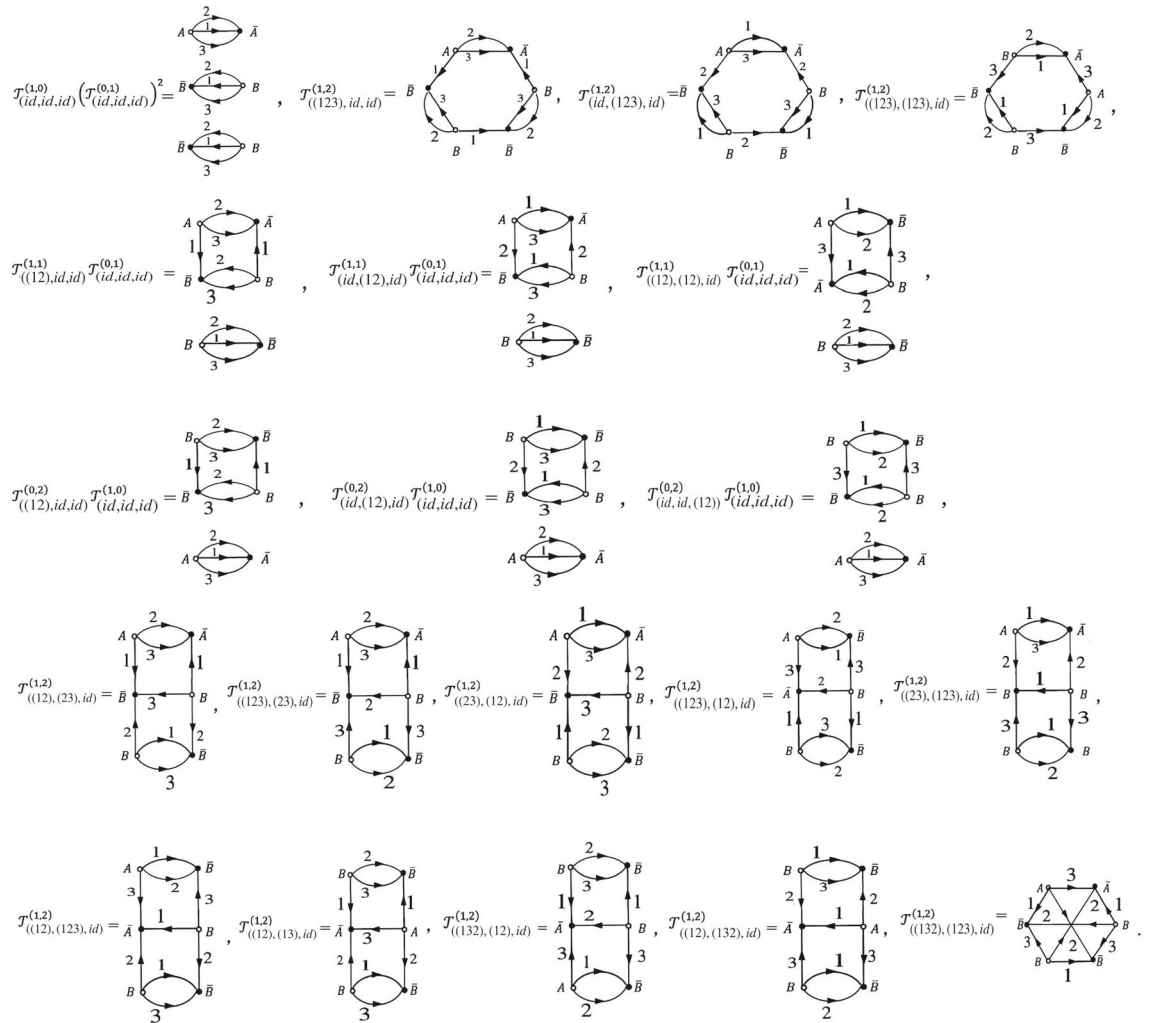
Fig. 6 Twenty operators in the case of $n = 1$ and $m = 2$ in (2.10)

where the second sum below over p is performed over all partitions of l [26]. From the following relation between disconnected operators and connected operators,

$$\eta(q) = 1 + \sum_{l=1}^{\infty} \sharp_l q^l = \mathrm{PE}(\eta^{conn}(q)) = \mathrm{PE}\left(\sum_{l=1}^{\infty} \sharp_l^{conn} q^l\right)$$
$$= \prod_{l=1}^{\infty} \frac{1}{(1 - q^l)^{\sharp_l^{conn}}}, \qquad (2.12)$$

the number $\sharp_l^{conn}$ can be read off from the plethystic logarithm

$$\mathrm{PLog}((\eta(q))) = \sum_{l=1}^{\infty} \sharp_l^{conn} q^l = \sum_{m=1}^{\infty} \frac{\mu(m)}{m} \log \eta(q^m), \qquad (2.13)$$

where $\mu(m)$ is the Möbius function

$$\mu(m) = \begin{cases} 0, & m \text{ has at least one repeated prime factor,} \\ 1, & m = 1, \\ (-1)^n, & m \text{ is a product of } n \text{ distinct primes.} \end{cases} \qquad (2.14)$$

2.3 Cut and join structure

Let us now discuss the kernel and cokernel of the cut-and-join structure in the ring $\mathcal{S}$. Due to the symmetry of Δ and $\tilde{\Delta}$ (or $\{,\}_A$ and $\{,\}_B$), we only focus on the cases Δ and $\{,\}_A$ here.

Since Δ maps all the operators at level-$(n+m)$ to those at level-$(n+m-1)$, Δ inevitably has a kernel [26]
$$\text{Ker}(\Delta) = \{\mathcal{T}_{\vec{\sigma}}^{(n,m)} \in \mathcal{S}_{n+m} | \Delta(\mathcal{T}_{\vec{\sigma}}^{(n,m)}) = 0\} \in \mathcal{S}_{n+m},$$
$$(2.15)$$

where $\mathcal{S}_{n+m}$ denotes the grading $n+m$ part of the ring $\mathcal{S}$. Due to the cokernel, there are many operators which are not the descendants produced only by join operation of keystones. It prevents the direct construction of the non-perturbed RG-complete partition function.

In what follows, we take the rings $\mathcal{S}_2$ and $\mathcal{S}_3$ as examples. In the ring $\mathcal{S}_2$, there are three disconnected gauge-invariant operators $(\mathcal{T}_{(id,id,id)}^{(1,0)})^2$, $\mathcal{T}_{(id,id,id)}^{(1,0)} \mathcal{T}_{(id,id,id)}^{(0,1)}$, $\mathcal{T}_{(id,id,id)}^{(0,1)} \mathcal{T}_{(id,id,id)}^{(0,1)}$ and nine connected gauge-invariant operators $\mathcal{T}_{((12),id,id)}^{(2,0)}$, $\mathcal{T}_{((12),id,id)}^{(0,2)}$, $\mathcal{T}_{(id,(12),id)}^{(2,0)}$, $\mathcal{T}_{(id,id,(12))}^{(2,0)}$, $\mathcal{T}_{(id,id,(12))}^{(2,0)}$, $\mathcal{T}_{(id,id,(12))}^{(0,2)}$, $\mathcal{T}_{(id,id,id)}^{(1,1)}$, $\mathcal{T}_{(id,(12),id)}^{(1,1)}$, $\mathcal{T}_{((12),(12),id)}^{(1,1)}$. The cut operation Δ takes operators from $\mathcal{S}_2$ to level-1 operators $\mathcal{T}_{(id,id,id)}^{(1,0)}$ and $\mathcal{T}_{(id,id,id)}^{(0,1)}$. In this case, through calculations we know that Δ has a kernel (of codimension two) with dimension ten
$$\text{ker}^{(2)}(\Delta) = \text{span}\{\mathcal{T}_{((12),id,id)}^{(0,2)}, \mathcal{T}_{(id,(12),id)}^{(0,2)},$$
$$\mathcal{T}_{(id,id,(12))}^{(0,2)}, \mathcal{T}_{(id,id,id)}^{(0,1)} \mathcal{T}_{(id,id,id)}^{(0,1)},$$
$$(\beta+1)\mathcal{T}_{((12),id,id)}^{(2,0)} - \alpha(\mathcal{T}_{(id,id,id)}^{(1,0)})^2,$$
$$(\beta+1)\mathcal{T}_{(id,(12),id)}^{(2,0)} - \tilde{\alpha}(\mathcal{T}_{(id,id,id)}^{(1,0)})^2,$$
$$(\beta+1)\mathcal{T}_{(id,id,(12))}^{(2,0)} - \hat{\alpha}(\mathcal{T}_{(id,id,id)}^{(1,0)})^2,$$
$$N_2 N_3 \mathcal{T}_{((12),(12),id)}^{(1,1)} - N_3 \mathcal{T}_{((12),id,id)}^{(1,1)},$$
$$N_1 N_3 \mathcal{T}_{((12),(12),id)}^{(1,1)} - N_3 \mathcal{T}_{(id,(12),id)}^{(1,1)},$$
$$\beta \mathcal{T}_{((12),(12),id)}^{(1,1)} - N_3 \mathcal{T}_{(id,id,id)}^{(1,0)} \mathcal{T}_{(id,id,id)}^{(0,1)}\}, \qquad (2.16)$$

where $\alpha = N_1 + N_2 N_3$, $\beta = N_1 N_2 N_3$, $\tilde{\alpha} = N_2 + N_1 N_3$ and $\hat{\alpha} = N_3 + N_1 N_2$.

In the following discussion, we omit the operators involving only field B and $\bar{B}$, since they are obviously included in kernel. Thus in $\mathcal{S}_3$, we only consider the gauge-invariant operators $\mathcal{T}_{((123),(132),id)}^{(3,0)}$, $\mathcal{T}_{((123),(132),id)}^{(2,1)}$ and the level-3 operators produced by join operation $\{,\}_A$ (see Table 2).

The cut operation Δ acting on the above level-3 gauge-invariant operators are listed in (A.1). Then we can give the kernel $\text{ker}^{(3)}(\Delta)$ with dimension 29 (see (A.2)) and cokernel as follows
$$\text{Coker}^{(3)}(\{,\}_A) = \text{span}\{\mathcal{T}_{((123),(132),id)}^{(3,0)}, \mathcal{T}_{((123),(132),id)}^{(2,1)}\}.$$
$$(2.17)$$

2.4 Join operators and Fredkin spin chain

The Fredkin spin chain [39,40] is a spin chain of length-$2n$, where up and down spin degrees of freedom with multiplicity (called as color) s are assigned at each of the lattice sites $\{1, 2, \ldots, 2n\}$. There is the connection between the Fredkin spin chain and large N matrix models [41]. The Hamiltonian of Fredkin spin chain is

$$H_{F,s} = \frac{1}{2} \sum_{j=1}^{2n-2} \sum_{k_1,k_2,k_3=1}^{s} \left\{ (|u_j^{k_1}, u_{j+1}^{k_2}, d_{j+2}^{k_3}\rangle \right.$$
$$- |u_j^{k_1}, d_{j+1}^{k_2}, u_{j+2}^{k_3}\rangle)(\langle u_j^{k_1}, u_{j+1}^{k_2}, d_{j+2}^{k_3}|$$
$$- \langle u_j^{k_1}, d_{j+1}^{k_2}, u_{j+2}^{k_3}|) + (|u_j^{k_1}, d_{j+1}^{k_2}, d_{j+2}^{k_3}\rangle$$
$$- |d_j^{k_1}, u_{j+1}^{k_2}, d_{j+2}^{k_3}\rangle)(\langle u_j^{k_1}, d_{j+1}^{k_2}, d_{j+2}^{k_3}|$$
$$\left. - \langle d_j^{k_1}, u_{j+1}^{k_2}, d_{j+2}^{k_3}| \right\}$$
$$+ \sum_{j=1}^{2n-1} \sum_{k\neq l} \left\{ |u_j^k, d_{j+1}^l\rangle\langle u_j^k, d_{j+1}^l| \right.$$
$$+ \frac{1}{2}(|u_j^k, d_{j+1}^k\rangle - |u_j^l, d_{j+1}^l\rangle)$$
$$\left. \times (\langle u_j^k, d_{j+1}^k| - \langle u_j^l, d_{j+1}^l|) \right\}$$
$$+ \sum_{k=1}^{s} \{|d_1^k\rangle\langle d_1^k| + |u_{2n}^k\rangle\langle u_{2n}^k|\}, \qquad (2.18)$$

where we express the up- and down-spin states with color $k \in \{1, 2, \ldots, s\}$ at the site i as $|u_i^k\rangle$ and $|d_i^k\rangle$, respectively. For the von Neumann entropy of the Fredkin model, it shows a square-root violation of the area law, and the scaling behavior of the first gap [39].

In this paper, we only focus on the case of $s = 2$ in (2.18). Thus the up- and down-spin states can be represented as arrows with color degrees of freedom in the two-dimensional (x, y)-plane pointing to $(1, 1)$ (up-step) and $(-1, -1)$ (down-step), respectively. For the Hamiltonian (2.18), it has a unique ground state at zero energy, which is superposition of spin configurations with equal weight. Each spin configuration appearing in the superposition is identified with each path of length-$2n$ Dyck walks. For the Dyck walks, they are random walks starting at the origin, ending at $(2n, 0)$ and restricted to the region $y \geqslant 0$. Furthermore the color of each up-step should be matched with that of the down-step subsequently appearing at the same height.

The ground state of the Fredkin spin chain is given by
$$|P_{F,2n,2}\rangle = \frac{1}{\sqrt{N_{F,2n,2}}} \sum_{\omega \in P_{F,2n,2}} |\omega\rangle, \qquad (2.19)$$

where $P_{F,2n,2}$ denotes the formal sum of length-$2n$ colored Dyck walks, ω runs over monomials appearing in $P_{F,2n,2}$,

Table 2 Level-3 operators produced by join operation $\{\ ,\ \}_A$

$\{\ ,\ \}_A$	$\mathcal{T}^{(2,0)}_{((12),id,id)}$	$\mathcal{T}^{(2,0)}_{(id,(12),id)}$	$\mathcal{T}^{(2,0)}_{(id,id,(12))}$	$\left(\mathcal{T}^{(1,0)}_{(id,id,id)}\right)^2$	$\mathcal{T}^{(1,1)}_{((12),id,id)}$	$\mathcal{T}^{(1,1)}_{(id,(12),id)}$	$\mathcal{T}^{(1,1)}_{((12),(12),id)}$	$\mathcal{T}^{(0,1)}_{(id,id,id)}\,\mathcal{T}^{(0,1)}_{(id,id,id)}$
$\mathcal{T}^{(2,0)}_{((12),id,id)}$	$4\mathcal{T}^{(3,0)}_{((123),id,id)}$							
$\mathcal{T}^{(2,0)}_{(id,(12),id)}$	$4\mathcal{T}^{(3,0)}_{((23),(12),id)}$	$4\mathcal{T}^{(3,0)}_{(id,(123),id)}$						
$\mathcal{T}^{(2,0)}_{(id,id,(12))}$	$4\mathcal{T}^{(3,0)}_{((123),(23),id)}$	$4\mathcal{T}^{(3,0)}_{((23),(123),id)}$	$4\mathcal{T}^{(3,0)}_{(id,id,(123))}$					
$\left(\mathcal{T}^{(1,0)}_{(id,id,id)}\right)^2$	$4\mathcal{T}^{(2,0)}_{((12),id,id)}\mathcal{T}^{(1,0)}_{(id,id,id)}$	$4\mathcal{T}^{(2,0)}_{(id,(12),id)}\mathcal{T}^{(1,0)}_{(id,id,id)}$	$4\mathcal{T}^{(2,0)}_{(id,id,(12))}\mathcal{T}^{(1,0)}_{(id,id,id)}$	$4\left(\mathcal{T}^{(1,0)}_{(id,id,id)}\right)^3$				
$\mathcal{T}^{(1,1)}_{((12),id,id)}$	$2\mathcal{T}^{(2,1)}_{((123),id,id)}$	$2\mathcal{T}^{(2,1)}_{((12),(23),id)}$	$2\mathcal{T}^{(2,1)}_{((132),(13),id)}$	$2\mathcal{T}^{(1,1)}_{((12),id,id)}\mathcal{T}^{(1,0)}_{(id,id,id)}$	$\mathcal{T}^{(1,2)}_{((123),id,id)}$			
$\mathcal{T}^{(1,1)}_{(id,(12),id)}$	$2\mathcal{T}^{(2,1)}_{((23),(12),id)}$	$2\mathcal{T}^{(2,1)}_{(id,(123),id)}$	$2\mathcal{T}^{(2,1)}_{((13),(132),id)}$	$2\mathcal{T}^{(1,1)}_{(id,(12),id)}\mathcal{T}^{(1,0)}_{(id,id,id)}$	$\mathcal{T}^{(1,2)}_{((23),(12),id)}$	$\mathcal{T}^{(1,2)}_{(id,(123),id)}$		
$\mathcal{T}^{(1,1)}_{((12),(12),id)}$	$2\mathcal{T}^{(2,1)}_{((123),(23),id)}$	$2\mathcal{T}^{(2,1)}_{((23),(123),id)}$	$2\mathcal{T}^{(2,1)}_{((123),(123),id)}$	$2\mathcal{T}^{(1,1)}_{((12),(12),id)}\mathcal{T}^{(1,0)}_{(id,id,id)}$	$\mathcal{T}^{(1,2)}_{((123),(23),id)}$	$\mathcal{T}^{(1,2)}_{((23),(123),id)}$	$\mathcal{T}^{(1,1)}_{((12),(12),id)}\mathcal{T}^{(0,1)}_{(id,id,id)}$	
$\mathcal{T}^{(1,0)}_{(id,id,id)}\mathcal{T}^{(0,1)}_{(id,id,id)}$	$2\mathcal{T}^{(2,0)}_{((12),id,id)}\mathcal{T}^{(0,1)}_{(id,id,id)}$	$2\mathcal{T}^{(2,0)}_{(id,(12),id)}\mathcal{T}^{(0,1)}_{(id,id,id)}$	$2\mathcal{T}^{(2,0)}_{(id,id,(12))}\mathcal{T}^{(0,1)}_{(id,id,id)}$	$2\left(\mathcal{T}^{(1,0)}_{(id,id,id)}\right)^2\mathcal{T}^{(0,1)}_{(id,id,id)}$	$\mathcal{T}^{(1,1)}_{((12),id,id)}\mathcal{T}^{(0,1)}_{(id,id,id)}$	$\mathcal{T}^{(1,1)}_{(id,(12),id)}\mathcal{T}^{(0,1)}_{(id,id,id)}$	$\mathcal{T}^{(1,1)}_{((12),(12),id)}\mathcal{T}^{(0,1)}_{(id,id,id)}$	$\mathcal{T}^{(1,0)}_{(id,id,id)}\left(\mathcal{T}^{(0,1)}_{(id,id,id)}\right)^2$

and $N_{F,2n,2}$ counts the number of the length-$2n$ colored Dyck walks

$$N_{F,2n,2} = 2^n N_{F,2n} = \frac{2^n}{n+1}\binom{2n}{n}, \tag{2.20}$$

where $N_{F,2n}$ denotes the n-th Catalan number.

Let us take $n = 2$ as an example, we have $N_{F,4,2} = 8$ and

$$\begin{aligned}|P_{F,2n,2}\rangle = \frac{1}{2\sqrt{2}}(&|u^1 d^1 u^2 d^2\rangle + |u^2 d^2 u^1 d^1\rangle \\ &+ |u^1 u^2 d^2 d^1\rangle + |u^2 u^1 d^1 d^2\rangle).\end{aligned} \tag{2.21}$$

The four states of the summand can be drawn as the colored Dyck walks (see Fig. 7).

In the previous subsection, we have presented the tree operators which are constructed by the keystone operators through the join operation. Since the gauge invariants $\mathcal{T}^{(n,m)}_{\check{\sigma}}$ with fixed positive integers n, m constitute the

double coset $H_{n,m} \backslash S_{n+m} \times S_{n+m} \times H_{n,m}/H_{n,m}$, there is $\check{\sigma} \cong (h_1\sigma_1 h_2, h_1\sigma_2 h_2, h_1\sigma_3 h_2)$, where $h_1, h_2 \in H_{n,m}$. If there exist h_1, h_2 such that $h_1\sigma_1 h_2 = id$ and $h_1\sigma_2 h_2$ is in the conjugacy class of $(1, 2, \ldots, n+m)$, we obtain the conjugacy class in which the Feynman diagrams are **I**–**II** cycles with shortcuts of color 3. When the shortcuts are disjoint, the Feynman diagrams represent the tree operators (see Fig. 2c, d).

Let us now establish the correspondence between two colored Dyck walks with length-$2(n+m)$ in Fredkin spin chain and tree operators. By cutting tree operators from lines of color 2, it gives a **I** or **II** segment with elements connected by disjoint lines of color 3, where each line of color 3 may correspond a up- and down-step. If the line of color 3 connects A and $\bar{A}$, we paint the step with purple, otherwise with yellow. We make the correspondence rule as follows:

(i) For the tree operators with rotational symmetry, we cut the fundamental domain of Feynman diagrams. For example, the Feynman diagram of $\mathcal{T}^{(2,2)}_{((1324),id,id)}$ has 2-fold rotation symmetry. Thus we only need to cut two lines color 2 connecting A and $\bar{A}$, B and $\bar{B}$, respectively (see left-hand side of Fig. 8). The segments **I** and **II** are shown in the middle parts of Fig. 8. Each line of color 3 in chains corresponds a up- and down-step in Dyck walks (see right-hand side of Fig. 8).

(ii) For the tree operators without rotational symmetry, we cut them from each line of color 1 or 2 (see examples in Figs. 9 and 10).

Here for the rotational symmetry of tree operators $\mathcal{T}^{(n,m)}_{\check{\sigma}}$, it means that there exist the disjoint d-cycles $\omega_1, \ldots, \omega_j$, $(d \times j = n + m)$, such that the following relations hold

$$\mathcal{T}^{(n,m)}_{(\omega_1\omega_2\cdots\omega_j \circledast \sigma_1 \circledast (\omega_1\omega_2\cdots\omega_j)^{-1},\,\omega_1\omega_2\cdots\omega_j \circledast \sigma_2 \circledast (\omega_1\omega_2\cdots\omega_j)^{-1},\,\omega_1\omega_2\cdots\omega_j \circledast \sigma_3 \circledast (\omega_1\omega_2\cdots\omega_j)^{-1})} = \mathcal{T}^{(n,m)}_{\check{\sigma}}, \tag{2.22}$$

where the symbol "$\circledast$" represents the composition of maps. Then we call the maximum value of d the fold of rotational symmetry of $\mathcal{T}^{(n,m)}_{\check{\sigma}}$.

From such correspondence, we see that $N_{F,2(n+m),2}$ counts the weight $\frac{n+m}{r}$ of tree operators with level-$(m+n)$, where r denotes the fold of rotational symmetry,
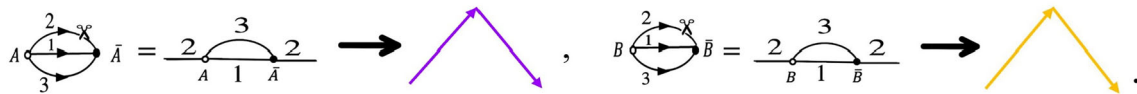
$$\begin{aligned}N_{F,2(n+m),2} &= 2^{(n+m)} N_{F,2(n+m)} = \frac{2^{n+m}}{n+m+1}\binom{2(n+m)}{n+m} \\ &= \sum_{i=1}^{\sharp^{tree}_{n+m}}\left(\text{weight of tree operator } \mathcal{T}^{(n,m)}_{\check{\alpha}_i}\right).\end{aligned} \tag{2.23}$$
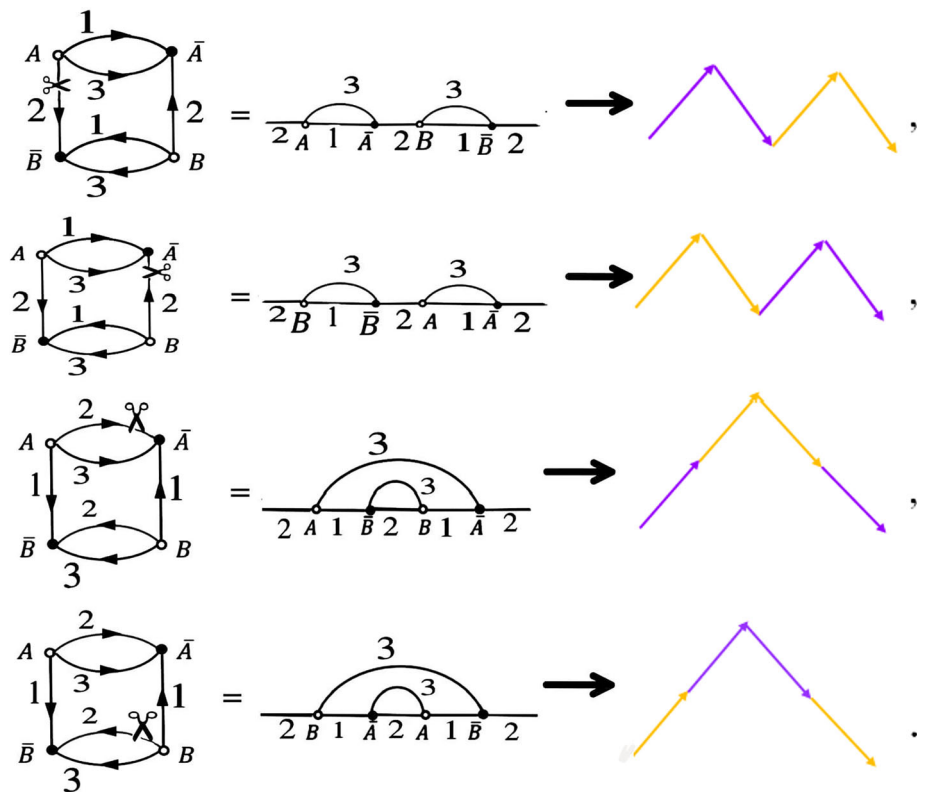
Fig. 7 Colored Dyck walks in the summand of (2.21)
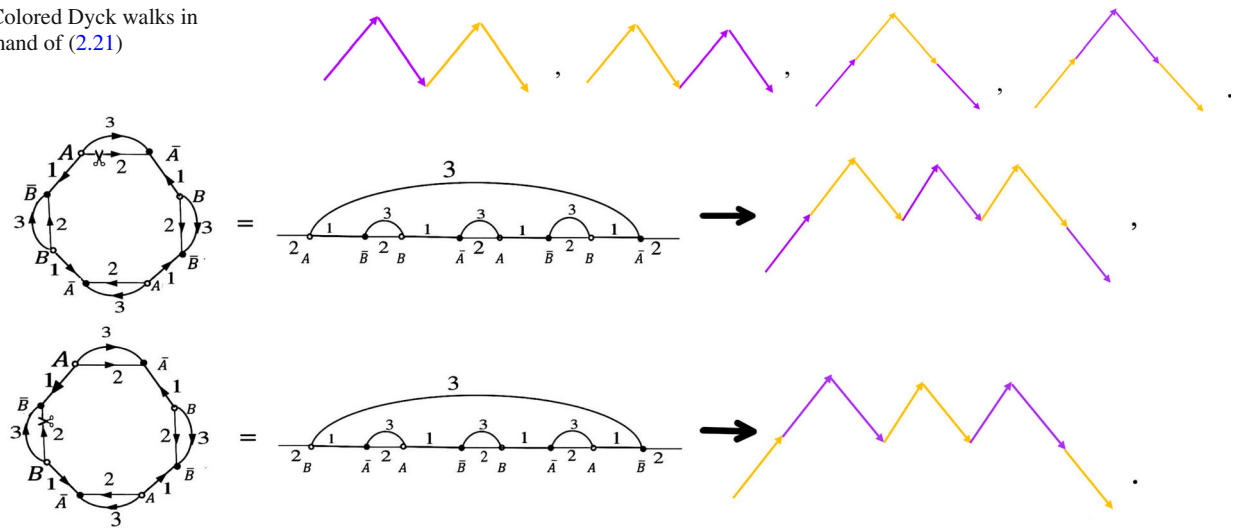
Fig. 8 Correspondence between $\mathcal{T}^{(2,2)}_{((1324),id,id)}$ and length-8 Dyck walks

Fig. 9 Correspondence between $\mathcal{T}^{(1,0)}_{(id,id,id)}$, $\mathcal{T}^{(0,1)}_{(id,id,id)}$ and length-2 Dyck walks

Fig. 10 Correspondence between $\mathcal{T}^{(1,1)}_{(id,(12),id)}$, $\mathcal{T}^{(1,1)}_{((12),id,id)}$ and length-4 Dyck walks

Then from (2.23), we obtain a partition $(n_1, n_2, \ldots, n_{\sharp_{n+m}^{tree}})$ of $N_{F,2(n+m),2}$, where $\sharp_{n+m}^{tree}$ denotes the number of tree operators with level-$(n + m = l)$. This partition gives a classification of length-$2(n + m)$ Dyck walks. Let us number the steps of Dyck walks. Then we move the first two steps to the back in turn and remain the matching relation (see examples in Fig. 11). By repeating the process above, we may obtain all Dyck walks belonging the same class, i.e., corresponding to the same tree operator cutted from different lines of color 2.

Based on the classification Dyck walks, it is easy to give the number of tree operators with level-l

$$\sharp_l^{tree} = \frac{N_{F,2l,2} + \sum_{i=1}^{l-1} \sum_r \frac{r-1}{r} l l_r + 2[2(l-1) + \sum_q \frac{q-1}{q} l l_q]}{l},$$

(2.24)

where r is the common factor of i and $l - i$, q is the factor of l, l_r and l_q count the number of Dyck walks with length r and q, respectively.

Since the number of connected operators with level-l, $\sharp_l^{conn}$, can be calculated from (2.12), we have the number of connected loop operators with level-l, $\sharp_l^{loop} = \sharp_l^{conn} - \sharp_l^{tree}$.

To divide the cutted Feynman diagram into two parts, we draw a vertical line passing the cutted line. It gives $(n + m - r)$ and $(n + m + r)$ fields in the left and right parts, respectively. Thus the corresponding two colored Dyck walks are divided into two subsystems, $\mathcal{A}$ with $(n + m - r)$, and $\mathcal{B}$ with $(n + m + r)$ spins, respectively. The spin configurations in subsystem $\mathcal{A}$ correspond to a part of colored Dyck paths from the origin to $(n + m + r, h)$ in the (x, y)-plane, and the spin configurations in subsystem $\mathcal{B}$ correspond to the paths from $(n + m + r, h)$ to $(2(n + m), 0)$. The part of $\mathcal{A}$ has h unmatched up-steps that are supposed to be matched across the boundary with h unmatched down-steps in the part of $\mathcal{B}$. For example, the cutted Feynman diagrams of $\mathcal{T}_{((12),id,id)}^{(1,1)}$ correspond to the Dyck walks of $n = m = 1$, $r = 0$ and $h = 2$ (see Fig. 12).

Let us denote the number of the paths in subsystem $\mathcal{A}$ as $N_{F,n+m+r,2}^{(0 \to h)}$, and the number of the paths in subsystem $\mathcal{B}$ as $N_{F,n+m-r,2}^{(h \to 0)}$. The correspondence implies that, $N_{F,n+m+r,2}^{(0 \to h)} N_{F,n+m-r,2}^{(h \to 0)}$ counts the number of cutted Feynman diagrams with h intersection points of the vertical line and lines of color 3, where

$$N_{F,n+m+r,2}^{(0 \to h)} = N_{F,n+m-r,2}^{(h \to 0)} = 2^\rho N_{F,n+m+r}^{(h)}$$
$$= \begin{cases} 2^\rho \frac{h+1}{\rho+1} \binom{n+m+r}{\rho}, & \rho \in \mathbb{N}, \\ 0, & otherwise. \end{cases}$$

(2.25)

The entanglement entropy of the quantum system divided into two systems is given by

$$s_{F,A} = - \sum_{h=0}^{n+m-|r|} 2^h p_{F,n+m+r,n+m-r,2}^{(h)} \ln p_{F,n+m+r,n+m-r,2}^{(h)},$$

(2.26)

where

$$p_{F,n+m+r,n+m-r,2}^{(h)} = 2^{-2h} \frac{N_{F,n+m+r,2}^{(0 \to h)} N_{F,n+m-r,2}^{(h \to 0)}}{N_{F,2(n+m),2}}.$$

(2.27)

For the entanglement entropy of the Fredkin spin chain, it exhibits a nonlogarithmic violation of the area law, which is beyond logarithmic scaling in the ordinary critical systems [39].

The ratio (2.27) plays an important role in the entanglement entropy. Note that $p_{F,n+m+r,m+n-r,2}^{(n+m-|r|)}$ is always the smallest in all $p_{F,n+m+r,n+m-r,2}^{(h)}$ for $n + m \geqslant 2$, since there is only the contribution from the diagrams with vertical line intersecting all possible lines of color 3 (see examples in Fig. 13). It prohibits all possible $p_{F,n+m+r,n+m-r,2}^{(h)}$ to be equal. Hence we conclude that the following relation does not hold

$$s_{F,A} = - \sum_{h=0}^{n+m-|r|} 2^h p_{F,n+m+r,n+m-r,2}^{(h)} \ln p_{F,n+m+r,n+m-r,2}^{(h)}$$
$$= - \sum_{i=1}^{k} 2^h \left(2^{-2h} \frac{1}{k}\right) \ln \left(2^{-2h} \frac{1}{k}\right) = 2^{-h} \ln 2^{2h} k,$$

(2.28)

where $k = [n + m - |r|] + 1$ due to the construction of tree operator. Thus we explain the entanglement scaling beyond logarithmic scaling in the ordinary critical systems from the viewpoint of tensor model here.

3 A two-tensor model with order-3

### 3.1 W-representation of the two-tensor model with order-3

We may choose keystone operators constructed from (2.3) to generate a renormalization group completed two-tensor model with order-3

$$Z_{AB} = \int dA d\bar{A} \int dB d\bar{B} \exp(-\text{Tr}A\bar{A} - \text{Tr}B\bar{B}$$
$$+ \sum_{n+m=1}^{\infty} \sum_{\check{\sigma} | \text{ level}(\check{\sigma})=n+m} N^{-2(n+m)} t_{\check{\sigma}}^{(n,m)} \mathcal{T}_{\check{\sigma}}^{(n,m)}),$$
$$= \int dA d\bar{A} \int dB d\bar{B} \exp(-\text{Tr}A\bar{A} - \text{Tr}B\bar{B}$$
$$+ N^{-2} t_{(id,id,id)}^{(1,0)} \mathcal{T}_{(id,id,id)}^{(1,0)} + N^{-2} t_{(id,id,id)}^{(0,1)} \mathcal{T}_{(id,id,id)}^{(0,1)}$$
$$+ \sum_{k=2}^{\infty} N^{-2k} t_{((12 \cdots k),id,id)}^{(k,0)} \mathcal{T}_{((12 \cdots k),id,id)}^{(k,0)}$$

Fig. 11 Two examples of moving the first two steps of Dyck walks to the back in turn
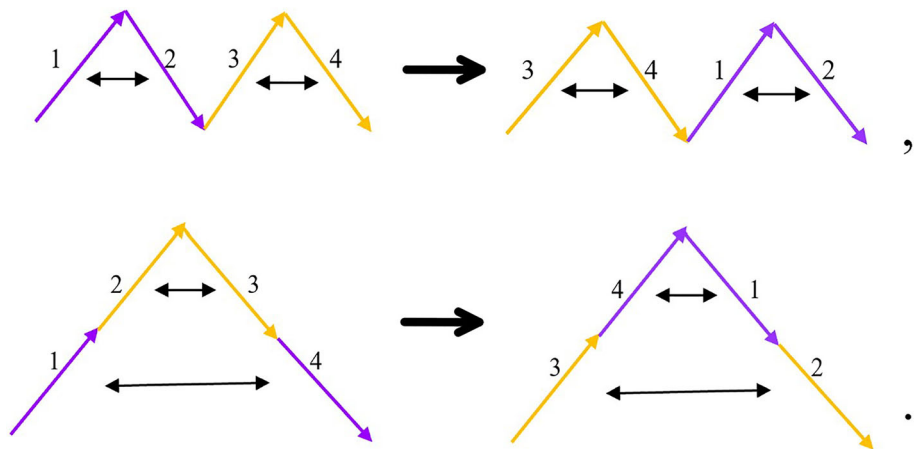
Fig. 12 Divide the cutted Feynman diagram of $\mathcal{T}_{((12),id,id)}^{(1,1)}$ into two parts, and two colored Dyck walks of two subsystems in the case of $n = m = 1$, $r = 0$ and $h = 2$
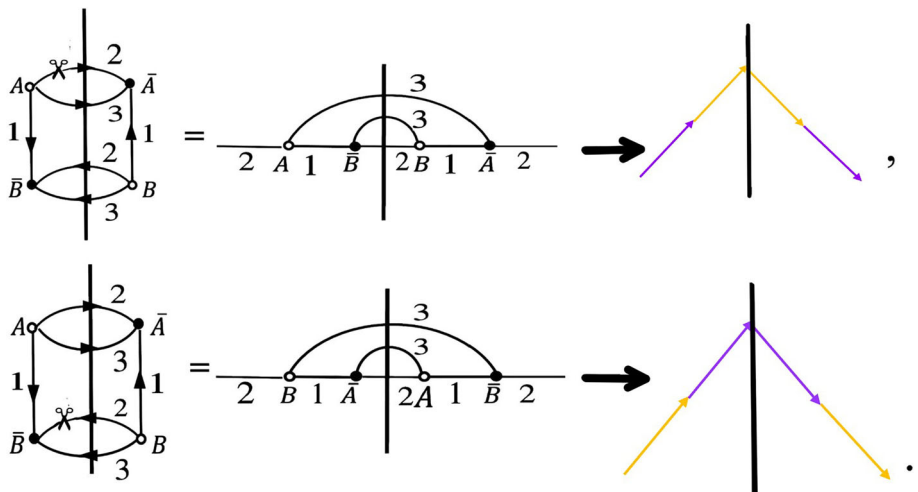
$$+ \sum_{k=2}^{\infty} N^{-2k} t_{((12\cdots k),id,id)}^{(0,k)} \mathcal{T}_{((12\cdots k),id,id)}^{(0,k)}$$

$$+ \sum_{k=2}^{\infty} N^{-2k} t_{(id,(12\cdots k),id)}^{(k,0)} \mathcal{T}_{(id,(12\cdots k),id)}^{(k,0)}$$

$$+ \sum_{k=2}^{\infty} N^{-2k} t_{(id,(12\cdots k),id)}^{(0,k)} \mathcal{T}_{(id,(12\cdots k),id)}^{(0,k)}$$

$$+ \sum_{k=2}^{\infty} N^{-2k} t_{(id,(12\cdots k),id)}^{(k,0)} \mathcal{T}_{(id,(12\cdots k),id)}^{(k,0)}$$

$$+ \sum_{k=2}^{\infty} N^{-2k} t_{(id,(12\cdots k),id)}^{(0,k)} \mathcal{T}_{(id,(12\cdots k),id)}^{(0,k)} + \cdots),$$

$$(3.1)$$

where the measure is induced by the norm $\| \delta A \delta B \|^2 = \delta A_i^{j_1,j_2} \delta \bar{A}_{j_1,j_2}^i \delta B_i^{j_1,j_2} \delta \bar{B}_{j_1,j_2}^i$.

By requiring that the partition function (3.1) is invariant under the transformation $A \to A + \delta A$, where $\delta A = \sum_{a+b=1}^{\infty} \sum_{\check{\alpha}| \text{ level}(\check{\alpha})=a+b} N^{-2(a+b)} t_{\check{\alpha}}^{(a,b)} \frac{\partial \mathcal{T}_{\check{\alpha}}^{(a,b)}}{\partial \bar{A}}$, we have

$$\left[- \sum_{a+b=1}^{\infty} \sum_{\check{\alpha}| \text{ level}(\check{\alpha})=a+b} a N^{-2(a+b)} t_{\check{\alpha}}^{(a,b)} \mathcal{T}_{\check{\alpha}}^{(a,b)} \right.$$

$$+ \sum_{a+b=1}^{\infty} \sum_{\check{\alpha}| \text{ level}(\check{\alpha})=a+b} N^{-2(a+b)} t_{\check{\alpha}}^{(a,b)} \Delta \mathcal{T}_{\check{\alpha}}^{(a,b)}$$

$$+ \sum_{\substack{a+b=1, \check{\alpha}| \text{ level}(\check{\alpha})=a+b, \\ n+m=1 \check{\sigma}| \text{ level}(\check{\sigma})=n+m}}^{\infty} N^{-2(a+b)} N^{-2(n+m)} t_{\check{\alpha}}^{(a,b)} t_{\check{\sigma}}^{(n,m)}$$

$$\left. \times \{\mathcal{T}_{\check{\sigma}}^{(n,m)}, \mathcal{T}_{\check{\alpha}}^{(a,b)}\}_A \right] Z_{AB} = 0. \tag{3.2}$$
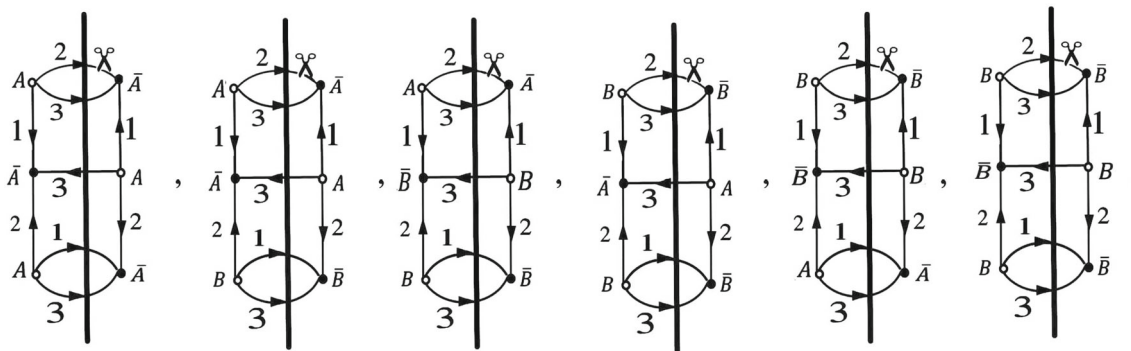
Fig. 13 The cutted Feynman diagrams contributing to $p_{F,3,3,2}^{(3)}$

Similarly, for the transformation $B \to B + \delta B$, where

$$\delta B = \sum_{a+b=1}^{\infty} \sum_{\check{\alpha}|\; \text{level}(\check{\alpha})=a+b} N^{-2(a+b)} t_{\check{\alpha}}^{(a+b)} \frac{\partial \mathcal{T}_{\check{\alpha}}^{(a,b)}}{\partial \bar{B}},$$ we have

$$\Bigg[-\sum_{a+b=1}^{\infty} \sum_{\check{\alpha}|\; \text{level}(\check{\alpha})=a+b} b N^{-2(a+b)} t_{\check{\alpha}}^{(a,b)} \mathcal{T}_{\check{\alpha}}^{(a,b)}$$

$$+ \sum_{a+b=1}^{\infty} \sum_{\check{\alpha}|\; \text{level}(\check{\alpha})=a+b} N^{-2(a+b)} t_{\check{\alpha}}^{(a,b)} \tilde{\Delta} \mathcal{T}_{\check{\alpha}}^{(a,b)}$$

$$+ \sum_{\substack{a+b=1,\; \check{\alpha}|\; \text{level}(\check{\alpha})=a+b, \\ n+m=1\; \check{\sigma}|\; \text{level}(\check{\sigma})=n+m}}^{\infty} N^{-2(a+b+n+m)} t_{\check{\alpha}}^{(a,b)} t_{\check{\sigma}}^{(n,m)}$$

$$\times \{\mathcal{T}_{\check{\sigma}}^{(n,m)}, \mathcal{T}_{\check{\alpha}}^{(a,b)}\}_B \Bigg] Z_{AB} = 0. \tag{3.3}$$

From (3.2) and (3.3), it is not difficult to obtain that the partition function (3.1) satisfies

$$\hat{D} Z_{AB} = \hat{W} Z_{AB}, \tag{3.4}$$

where

$$\hat{D} = \sum_{a+b=1}^{\infty} \sum_{\check{\alpha}|\; \text{level}(\check{\alpha})=a+b} a N^{-2(a+b)} t_{\check{\alpha}}^{(a,b)} \frac{\partial}{\partial t_{\check{\alpha}}^{(a,b)}}$$

$$+ \sum_{a+b=1}^{\infty} \sum_{\check{\alpha}|\; \text{level}(\check{\alpha})=a+b} b N^{-2(a+b)} t_{\check{\alpha}}^{(a,b)} \frac{\partial}{\partial t_{\check{\alpha}}^{(a,b)}}, \tag{3.5}$$

$$\hat{W} = \sum_{a+b=1}^{\infty} \sum_{\check{\alpha}|\; \text{level}(\check{\alpha})=a+b} \sum_{k=1}^{3} \sum_{\substack{\check{\beta}_1,\ldots,\check{\beta}_k, \\ a_1+\cdots+a_k+1=a, \\ b_1+\cdots+b_k=b, \\ asps_1 \leq a_2 \leq \cdots \leq a_k}} (1-\delta_{a,1})$$

$$\times \Delta_{\check{\alpha},\check{\beta}_1,\ldots,\check{\beta}_k}^{(a,b),(a_1,b_1),\ldots,(a_k,b_k)} N^{-2(a+b)} t_{\check{\alpha}}^{(a,b)}$$

$$\times \frac{\partial}{\partial t_{\check{\beta}_1}^{(a_1,b_1)}} \cdots \frac{\partial}{\partial t_{\check{\beta}_k}^{(a_k,b_k)}}$$

$$+ \sum_{a+b=1}^{\infty} \sum_{\check{\alpha}|\; \text{level}(\check{\alpha})=a+b} \sum_{k=1}^{3} \sum_{\substack{\check{\gamma}_1,\ldots,\check{\gamma}_k, \\ a_1+\cdots+a_k+1=a, \\ b_1+\cdots+b_k=b, \\ bsps_1 \leq b_2 \leq \cdots \leq b_k}} (1-\delta_{b,1})$$

$$\times \tilde{\Delta}_{\check{\alpha},\check{\gamma}_1,\ldots,\check{\gamma}_k}^{(a,b),(a_1,b_1),\ldots,(a_k,b_k)} N^{-2(a+b)} t_{\check{\alpha}}^{(a,b)}$$

$$\times \frac{\partial}{\partial t_{\check{\gamma}_1}^{(a_1,b_1)}} \cdots \frac{\partial}{\partial t_{\check{\gamma}_k}^{(a_k,b_k)}}$$

$$+ \sum_{\substack{a+b=1, \\ n+m=1}}^{\infty} \sum_{\substack{\check{\alpha}|\; \text{level}(\check{\alpha})=a+b, \\ \check{\sigma}|\; \text{level}(\check{\sigma})=n+m, \\ \check{\beta}|\; \text{level}(\check{\beta})=n+m+a+b-1}} \Lambda_{\check{\sigma},\check{\alpha},\check{\beta}}^{(n,m),(a,b),(n+a-1,m+b)}$$

$$\times N^{-2(a+b)} N^{-2(n+m)} t_{\check{\alpha}}^{(a,b)} t_{\check{\sigma}}^{(n,m)} \frac{\partial}{\partial t_{\check{\beta}}^{(n+a-1,m+b)}}$$

$$+ \sum_{\substack{a+b=1, \\ n+m=1}}^{\infty} \sum_{\substack{\check{\alpha}|\; \text{level}(\check{\alpha})=a+b, \\ \check{\sigma}|\; \text{level}(\check{\sigma})=n+m, \\ \check{\beta}|\; \text{level}(\check{\beta})=n+m+a+b-1}} \tilde{\Lambda}_{\check{\sigma},\check{\alpha},\check{\gamma}}^{(n,m),(a,b),(n+a-1,m+b)}$$

$$\times N^{-2(a+b)} N^{-2(n+m)} t_{\check{\alpha}}^{(a,b)} t_{\check{\sigma}}^{(n,m)} \frac{\partial}{\partial t_{\check{\gamma}}^{(n+a-1,m+b)}}$$

$$+ N^{-2} t_{(id,id,id)}^{(1,0)} \mathcal{N}_3 + N^{-2} t_{(id,id,id)}^{(0,1)} \mathcal{N}_3, \tag{3.6}$$

where $\breve{\alpha}$, $\breve{\beta}$ and $\breve{\sigma}$ are taken from indices of connected operators in the ring, $\mathcal{N}_3 = N_1 N_2 N_3$.

Let us rewrite (3.1) as

$$Z_{AB} = \sum_{s=0}^{\infty} Z_{AB}^{(s)}, \tag{3.7}$$

where

$$Z_{AB}^{(s)} = \int dA \, d\bar{A} \, dB \, d\bar{B} \, \exp(-\mathrm{Tr} A\bar{A} - \mathrm{Tr} B\bar{B})$$
$$\cdot \sum_{l=0}^{\infty} \sum_{\substack{\breve{\sigma}_i \mid \text{level}(\breve{\sigma}_i)=n_i+m_i, \\ n_1+m_1+\cdots+n_l+m_l=s}} \frac{1}{l!} \left\langle \prod_{i=1}^{l} \mathcal{T}_{\breve{\sigma}_i}^{(n_i,m_i)} \right\rangle$$
$$\cdot N^{-2(n_1+m_1+\cdots+n_l+m_l)} \prod_{i=1}^{l} t_{\breve{\sigma}_i}^{(n_i,m_i)}, \tag{3.8}$$

and the correlators $\langle \prod_{i=1}^{l} \mathcal{T}_{\breve{\sigma}_i}^{(n_i,m_i)} \rangle$ are defined by

$$\left\langle \prod_{i=1}^{l} \mathcal{T}_{\breve{\sigma}_i}^{(n_i,m_i)} \right\rangle = \frac{\int dA \, d\bar{A} \, dB \, d\bar{B} \, \mathcal{T}_{\breve{\sigma}_1}^{(n_1,m_1)} \mathcal{T}_{\breve{\sigma}_2}^{(n_2,m_2)} \cdots \mathcal{T}_{\breve{\sigma}_l}^{(n_l,m_l)} \exp(-\mathrm{Tr} A\bar{A} - \mathrm{Tr} B\bar{B})}{\int dA \, d\bar{A} \, dB \, d\bar{B} \, \exp(-\mathrm{Tr} A\bar{A} - \mathrm{Tr} B\bar{B})}. \tag{3.9}$$

From the operators $\hat{D}$ and $\hat{W}$ acting on $Z_{AB}^{(s)}$,

$$\hat{D} Z_{AB}^{(s)} = s Z_{AB}^{(s)}, \tag{3.10}$$
$$\hat{W} Z_{AB}^{(s)} = (s+1) Z_{AB}^{(s+1)}, \tag{3.11}$$

we see that the operators $\hat{D}$ and $\hat{W}$ are indeed the operators preserving and increasing the grading, respectively. Thus the partition function can be realized by the W-representation

$$Z_{AB} = \exp(\hat{W}) \cdot 1. \tag{3.12}$$

Let us write the k-th power of the operator $\hat{W}$ as

$$\hat{W}^k = \sum_{i=1}^{k} \sum_{a_1+b_1+\cdots+a_i+b_i=k} \sum_{\breve{\alpha}_i \mid \text{level}(\breve{\alpha}_i)=a_i+b_i} P_{\breve{\alpha}_1,\ldots,\breve{\alpha}_i}^{(a_1,b_1),\ldots,(a_i,b_i)}$$
$$\times N^{-2k} t_{\breve{\alpha}_1}^{(a_1,b_1)} \cdots t_{\breve{\alpha}_i}^{(a_i,b_i)}$$
$$+ \sum_{i=1}^{2k} \sum_{j=1}^{3k} \sum_{\substack{a_1+b_1\cdots+a_i+b_i \\ -n_1-m_1-\cdots-n_j-m_j=k}}$$
$$\times \sum_{\substack{\breve{\alpha}_i \mid \text{level}(\breve{\alpha}_i)=a_i+b_i, \\ \breve{\beta}_j \mid \text{level}(\breve{\beta}_j)=n_j+m_j}} P_{\breve{\alpha}_1,\ldots,\breve{\alpha}_i;(a_1,b_1),\ldots,(a_i,b_i)}^{\breve{\beta}_1,\ldots,\breve{\beta}_j;(n_1,m_1),\ldots,(n_j,m_j)}$$
$$\cdot N^{-2k} t_{\breve{\alpha}_1}^{(a_1,b_1)} \cdots t_{\breve{\alpha}_i}^{(a_i,b_i)} \frac{\partial}{\partial t_{\breve{\beta}_1}^{(n_1,m_1)}} \cdots \frac{\partial}{\partial t_{\breve{\beta}_j}^{(n_j,m_j)}}, \tag{3.13}$$

where the coefficients $P_{\breve{\alpha}_1,\ldots,\breve{\alpha}_i}^{(a_1,b_1),\ldots,(a_i,b_i)}$ and $P_{\breve{\alpha}_1,\ldots,\breve{\alpha}_i;(a_1,b_1),\ldots,(a_i,b_i)}^{\breve{\beta}_1,\ldots,\breve{\beta}_j;(n_1,m_1),\ldots,(n_j,m_j)}$ are polynomials of N_1, N_2 and N_3.

Then it is not difficult to derive the compact expression of correlators from (3.12)

$$\left\langle \mathcal{T}_{\breve{\alpha}_1}^{(a_1,b_1)} \cdots \mathcal{T}_{\breve{\alpha}_i}^{(a_i,b_i)} \right\rangle = \frac{i!}{k! \lambda_{(\breve{\alpha}_1,\ldots,\breve{\alpha}_i)}} \sum_{\tau} P_{\tau(\breve{\alpha}_1),\ldots,\tau(\breve{\alpha}_i)}^{(a_1,b_1),\ldots,(a_i,b_i)}, \tag{3.14}$$

where $k = a_1 + b_1 + \cdots + a_i + b_i$, τ denotes all distinct permutations of $(\breve{\alpha}_1, \ldots, \breve{\alpha}_i)$ and $\lambda_{(\breve{\alpha}_1,\ldots,\breve{\alpha}_i)}$ is the number of τ with respect to $\breve{\alpha}_1, \ldots, \breve{\alpha}_i$.

We list some correlators in (3.14) as follows:

$$\left\langle \mathcal{T}_{(id,id,id)}^{(1,0)} \right\rangle = \left\langle \mathcal{T}_{(id,id,id)}^{(0,1)} \right\rangle = \mathcal{N}_3,$$
$$\left\langle \mathcal{T}_{((12),id,id)}^{(2,0)} \right\rangle = \left\langle \mathcal{T}_{((12),id,id)}^{(0,2)} \right\rangle = \mathcal{N}_3(N_1 + N_2 N_3),$$
$$\left\langle \mathcal{T}_{(id,id,id)}^{(1,0)} \mathcal{T}_{(id,id,id)}^{(1,0)} \right\rangle = \left\langle \mathcal{T}_{(id,id,id)}^{(0,1)} \mathcal{T}_{(id,id,id)}^{(0,1)} \right\rangle = \mathcal{N}_3^2 + \mathcal{N}_3,$$
$$\left\langle \mathcal{T}_{(id,id,id)}^{(1,0)} \mathcal{T}_{(id,id,id)}^{(0,1)} \right\rangle = \mathcal{N}_3^2, \quad \left\langle \mathcal{T}_{((12),id,id)}^{(1,1)} \right\rangle = \mathcal{N}_3 N_2 N_3,$$

$$\left\langle \mathcal{T}_{(id,id,id)}^{(1,0)} \mathcal{T}_{((12),id,id)}^{(2,0)} \right\rangle = \left\langle \mathcal{T}_{(id,id,id)}^{(0,1)} \mathcal{T}_{((12),id,id)}^{(0,2)} \right\rangle$$
$$= \mathcal{N}_3(N_1 + N_2 N_3) + \mathcal{N}_3^2(N_1 + N_2 N_3),$$
$$\left\langle \mathcal{T}_{(id,id,id)}^{(1,0)} \mathcal{T}_{((12),id,id)}^{(0,2)} \right\rangle = \left\langle \mathcal{T}_{(id,id,id)}^{(0,1)} \mathcal{T}_{((12),id,id)}^{(2,0)} \right\rangle$$
$$= \mathcal{N}_3^2(N_1 + N_2 N_3),$$
$$\left\langle \mathcal{T}_{((123),id,id)}^{(3,0)} \right\rangle = \left\langle \mathcal{T}_{((123),id,id)}^{(0,3)} \right\rangle$$
$$= \mathcal{N}_3^2 + \mathcal{N}_3 + \mathcal{N}_3[N_1^2 + (N_2 N_3)^2 + 2N_1 N_2 N_3],$$
$$\left\langle \mathcal{T}_{(id,(123),(12))}^{(3,0)} \right\rangle = \left\langle \mathcal{T}_{(id,(123),(12))}^{(0,3)} \right\rangle$$
$$= \mathcal{N}_3^2 N_3 + \mathcal{N}_3(N_2^2 N_3 + N_1^2 N_3 + 2N_1 N_2 + N_3),$$
$$\left\langle \mathcal{T}_{(id,(123),(132))}^{(3,0)} \right\rangle = \left\langle \mathcal{T}_{(id,(123),(132))}^{(0,3)} \right\rangle$$
$$= 3\mathcal{N}_3^2 + \mathcal{N}_3(N_1^2 + N_2^2 + N_3^2),$$
$$\left\langle \mathcal{T}_{((123),id,id)}^{(2,1)} \right\rangle = \left\langle \mathcal{T}_{((123),id,id)}^{(1,2)} \right\rangle$$
$$= \mathcal{N}_3^2 + \mathcal{N}_3(N_2 N_3)^2,$$
$$\left\langle \mathcal{T}_{(id,(123),(12))}^{(2,1)} \right\rangle = \left\langle \mathcal{T}_{(id,(123),(12))}^{(1,2)} \right\rangle$$
$$= \mathcal{N}_3^2 N_3 + \mathcal{N}_3(N_2^2 N_3 + 2N_1 N_2 + N_3),$$
$$\left\langle \mathcal{T}_{(id,id,id)}^{(1,0)} \mathcal{T}_{(id,id,id)}^{(1,0)} \mathcal{T}_{(id,id,id)}^{(0,1)} \right\rangle$$
$$= \left\langle \mathcal{T}_{(id,id,id)}^{(1,0)} \mathcal{T}_{(id,id,id)}^{(0,1)} \mathcal{T}_{(id,id,id)}^{(0,1)} \right\rangle = \mathcal{N}_3^3 + \mathcal{N}_3^2,$$
$$\left\langle \mathcal{T}_{((12),id,id)}^{(1,1)} \mathcal{T}_{(id,id,id)}^{(1,0)} \right\rangle = \left\langle \mathcal{T}_{((12),id,id)}^{(1,1)} \mathcal{T}_{(id,id,id)}^{(0,1)} \right\rangle$$
$$= \mathcal{N}_3^2 N_2 N_3 + \mathcal{N}_3 N_2 N_3,$$
$$\left\langle (\mathcal{T}_{(id,id,id)}^{(1,0)})^i \right\rangle = \left\langle (\mathcal{T}_{(id,id,id)}^{(0,1)})^i \right\rangle = \prod_{j=0}^{i-1}(\mathcal{N}_3 + j). \tag{3.15}$$

3.2 Perturbative collective field theory

Let us consider the Hamiltonian [23]

$$H = -\frac{\partial}{\partial A_i^{j,k}}\frac{\partial}{\partial \bar{A}_i^{j,k}} - \frac{\partial}{\partial B_i^{j,k}}\frac{\partial}{\partial \bar{B}_i^{j,k}}$$
$$+ \frac{1}{4}A_i^{j,k}\bar{A}_i^{j,k} + \frac{1}{4}B_i^{j,k}\bar{B}_i^{j,k}. \tag{3.16}$$

We introduce the collective variables

$$\Phi_k = \text{Tr}(e^{ikT}), \tag{3.17}$$

where T is a matrix on the vector space with elements

$$T_{i_1}^{i_2} = A_{i_1}^{j_1,j_2}\bar{A}_{j_1,j_2}^{i_2} + B_{i_1}^{j_1,j_2}\bar{B}_{j_1,j_2}^{i_2}. \tag{3.18}$$

Note that it is different from the discussion in [23] where the second term in (3.18) was dropped.

Let us introduce the field $\Phi(x) = \int \frac{dk}{2\pi}e^{-ikx}\Phi_k$, which is the eigenvalues density of matrix T [22]. Using the collective variables Φ_k, we rewrite the kinetic terms in (3.16) as

$$-\frac{\partial}{\partial A_i^{j,k}}\frac{\partial}{\partial \bar{A}_i^{j,k}} - \frac{\partial}{\partial B_i^{j,k}}\frac{\partial}{\partial \bar{B}_i^{j,k}}$$
$$= -T_l^i\frac{\partial}{\partial T_l^j}\frac{\partial}{\partial T_i^j} - 2N_2N_3\frac{\partial}{\partial T_i^i}$$
$$= \int dk \int dk' \Omega_{k,k'}\pi_k\pi_{k'} + \int dk\omega_k\pi_k, \tag{3.19}$$

where $\pi_k = \frac{1}{i}\frac{\delta}{\delta\Phi_k}$, $\Omega_{k,k'}$ and ω_k are given by

$$\Omega_{k,k'} = T_l^i\frac{\partial\Phi_k}{\partial T_l^j}\frac{\partial\Phi_{k'}}{\partial T_i^j} = ikk'\frac{\partial}{\partial k}\Phi_{k+k'},$$

$$\omega_k = -T_l^i\frac{\partial}{\partial T_l^j}\left(\frac{\partial\Phi_k}{\partial T_i^j}\right) - 2N_2N_3\frac{\partial\Phi_k}{\partial T_i^i}$$
$$= k\int_0^1 d\tau\Phi_{(1-\tau)k} - 2ikN_2N_3\Phi_k. \tag{3.20}$$

Then by the fourier transformations of (3.20), we have

$$\Omega(x,x') = \partial_x\partial_{x'}(x\Phi(x)\delta(x-x')),$$
$$\omega(x) = 2\partial_x \fint dy\Phi(x)\Phi(y)\frac{x}{x-y}$$
$$+ [2N_2N_3 - N_1]\partial_x\Phi(x). \tag{3.21}$$

We may further write the Hamiltonian in terms of the collective variables. By performing similarity transformation on Hamiltonian to hermitian it, it gives an equality

$$2\int dx'\Omega(x,x',\Phi)C(x') + \omega(x,\Phi) = 0. \tag{3.22}$$

From (3.22), we have

$$\partial_x C(x) = \frac{1}{2x}\cdot\fint dy\frac{2x\Phi(y)}{x-y} + \frac{(2\cdot\frac{N_2N_3}{N_1} - 1)N_1}{2x}. \tag{3.23}$$

The desired Hamiltonian can be finally written as

$$H = \int dx\frac{\partial\pi(x)}{\partial x}\phi(x)\frac{\partial\pi(x)}{\partial x} + V_{eff}, \tag{3.24}$$

where $\pi(x) = \frac{1}{i}\frac{\delta}{\delta\Phi(x)}$, the effective potential is given by

$$V_{eff} = \int dx\left[\frac{\pi^2}{3}x\Phi(x)^3 + \frac{(2\cdot\frac{N_2N_3}{N_1} - 1)^2}{4x}N_1{}^2\Phi(x)\right.$$
$$\left. + \frac{x}{4}\Phi(x) - \Lambda\Phi(x)\right], \tag{3.25}$$

Λ is the lagrange multiplier enforces the constraint $\int dx\Phi(x) = N_1$.

The classical field should minimize the effective potential. By $\frac{\delta V_{eff}}{\delta\Phi} = 0$, we have

$$\pi^2x\Phi^2 + \frac{(2\cdot\frac{N_2N_3}{N_1} - 1)^2}{4x}N_1{}^2 + \frac{x}{4} - \Lambda = 0. \tag{3.26}$$

By requiring $2\Lambda - \sqrt{4\Lambda^2 - N_1{}^2} \leq x \leq 2\Lambda + \sqrt{4\Lambda^2 - N_1{}^2}$ and taking the limit $\frac{N_2N_3}{N_1} \to 1$ and the multiplier $\Lambda = \frac{3}{2}N_1$ in (3.26), we obtain the classical collective field

$$\Phi(x) = \frac{1}{2\pi}\sqrt{\frac{6N_1}{x} - 1 - \frac{N_1{}^2}{x^2}}. \tag{3.27}$$

Then the collective field computation gives

$$\int_{(3-2\sqrt{2})N_1}^{(3+2\sqrt{2})N_1} dx\Phi(x)x^n = C_nN_1{}^{n+1}, \tag{3.28}$$

where

$$C_n = 4\cdot 3^{n-1} - 6(1 + (-1)^n)\frac{(2\sqrt{2})^{n-2}(n-1)(n-1)!!}{n!!}$$
$$- 2(1 + (-1)^{n+1})\frac{(2\sqrt{2})^{n-1}n!!}{(n+1)!!}$$
$$+ 2\frac{(n-1)!!}{n!!}\sum_{k=2}^{n-1}(2\sqrt{2})^{k-2}3^{n-k-1}(1 + (-1)^k)$$
$$\times\left[8\binom{n-1}{k} - 9\binom{n-1}{k-2}\right]. \tag{3.29}$$

The first several ones of (3.28) are

$$\int_{(3-2\sqrt{2})N_1}^{(3+2\sqrt{2})N_1} dx\Phi(x)x = 2N_1{}^2,$$
$$\int_{(3-2\sqrt{2})N_1}^{(3+2\sqrt{2})N_1} dx\Phi(x)x^2 = 6N_1{}^3,$$
$$\int_{(3-2\sqrt{2})N_1}^{(3+2\sqrt{2})N_1} dx\Phi(x)x^3 = 22N_1{}^4. \tag{3.30}$$

As done in Ref. [22], let us consider the limit that $N_i \to \infty$, $(i = 1, 2, 3)$ and setting $N_1 = N_2N_3$ in the correlators $\langle\text{Tr}T^n\rangle$, then the classical collective solution (3.28) gives the

highest power term of N_1 in $\langle \mathrm{Tr} T^n \rangle$. Thus in this large N_i limit, we write the correlators as

$$\langle \mathrm{Tr} T^n \rangle = \langle \mathrm{Tr}(A\bar{A} + B\bar{B})^n \rangle = C_n N_1^{\,n+1} + \mathrm{o}(N_1^{\,n}), \quad (3.31)$$

where the expression of $\mathrm{Tr}(A\bar{A} + B\bar{B})^n$ contains all the tree operators $\mathcal{T}^{(p,n-p)}_{(\sigma,id,id)}, \sigma \in S_n$, in $\tilde{S}$, $\tilde{S}$ is a closed ring generated by $\mathcal{T}^{(2,0)}_{((12),id,id)}$, $\mathcal{T}^{(0,2)}_{((12),id,id)}$ and $\mathcal{T}^{(1,1)}_{((12),id,id)}$ through addition, multiplication, cut and join operations.

Let us list the correlators corresponding to (3.30)

simultaneous appear in these Feynman diagrams. We delete the lines index 3 in these Feynman diagrams (see examples in the left part of Fig. 14), which do not affect the results in this section. Thus the Wick contractions contributing to the highest power terms of N_1 in (3.32) can be depicted as circles **I** and **II** with disjoint dotted lines connecting A and $\bar{A}$, or B and $\bar{B}$, where dotted lines denote Wick contractions. Then by changing the dotted lines into lines of color 3, we obtain tree operators in the closed ring $\check{S}$ generated by five keystones $\mathcal{T}^{(2,0)}_{((12),id,id)}$, $\mathcal{T}^{(0,2)}_{((12),id,id)}$, $\mathcal{T}^{(2,0)}_{(id,(12),id)}$, $\mathcal{T}^{(0,2)}_{(id,(12),id)}$

$$\langle \mathrm{Tr} T \rangle = \left\langle \mathcal{T}^{(1,0)}_{(id,id,id)} \right\rangle + \left\langle \mathcal{T}^{(0,1)}_{(id,id,id)} \right\rangle$$

$$= 2N_1^{\,2},$$

$$\langle \mathrm{Tr} T^2 \rangle = \left\langle \mathcal{T}^{(2,0)}_{((12),id,id)} \right\rangle + \left\langle \mathcal{T}^{(0,2)}_{((12),id,id)} \right\rangle + 2\left\langle \mathcal{T}^{(1,1)}_{((12),id,id)} \right\rangle$$

$$= 6N_1^{\,3},$$

$$\langle \mathrm{Tr} T^3 \rangle = \left\langle \mathcal{T}^{(3,0)}_{((123),id,id)} \right\rangle + \left\langle \mathcal{T}^{(0,3)}_{((123),id,id)} \right\rangle + 3\left\langle \mathcal{T}^{(2,1)}_{((123),id,id)} \right\rangle + 3\left\langle \mathcal{T}^{(1,2)}_{((123),id,id)} \right\rangle$$

$$= 22 N_1^{\,4} + 2 N_1^{\,2} = 22 N_1^{\,4} + \mathrm{o}(N_1^{\,3}), \quad (3.32)$$

where the dotted lines depict the Feynman propagators.

The Feynman diagrams of operators in $\tilde{S}$ are circles **I** (see Fig. 3a). It implies that the lines of color 2 and 3 always

and $\mathcal{T}^{(1,1)}_{((12),id,id)}$ (see examples in the second part on the left of Fig. 14).

For the number of the length-$2n$ two colored Dyck walks, it is counted by 2^n multiples of the n-th Catalan number (2.20). Based on the correspondence between Fredkin spin chain and tree operators in the previous section, we see that the number of spin chains corresponding to tree operators with level-n in $\check{S}$ is given by C_n. In other words, C_n counts the number of special length-$2n$ two colored Dyck walks which satisfy the following two conditions: (i) The colors of the first and last steps are same. (ii) The colors of $2k$-th and $(2k+1)$-th steps are same, but for the $(2k-1)$-th and $2k$-th steps, $k = 1, 2, \ldots, n-1$, their colors don't have to be same. In Fig. 14, we take $\langle \text{Tr} T^2 \rangle$ in (3.32) as an example to draw the corresponding six spin chains.

3.3 Free energy and large N limit

Let us consider the free energy $\mathcal{F}$ of the two-tensor model (3.1)

$$
\begin{aligned}
\mathcal{F} &= -\ln Z_{AB} \\
&= \sum_{s,l=0}^{\infty} \sum_{\substack{\lambda \mapsto l, \, length(\lambda)=p, \\ \check{\alpha}_i \mid level(\check{\alpha}_i)=n_i+m_i, \\ n_1+m_1+\cdots+n_{\lambda_p}+m_{\lambda_p}=s}} \frac{(-1)^{p+1}}{l!p} S(\mu) \tilde{S}(\lambda) \\
&\quad \times \langle \mathcal{T}^{(n_1,m_1)}_{\check{\alpha}_1} \cdots \mathcal{T}^{(n_{\lambda_1},m_{\lambda_1})}_{\check{\alpha}_{\lambda_1}} \rangle \langle \mathcal{T}^{(n_{\lambda_1+1},m_{\lambda_1+1})}_{\check{\alpha}_{\lambda_1+1}} \cdots \mathcal{T}^{(n_{\lambda_2},m_{\lambda_2})}_{\check{\alpha}_{\lambda_2}} \rangle \\
&\quad \cdots \cdot \langle \mathcal{T}^{(n_{\lambda_{p-1}+1},m_{\lambda_{p-1}+1})}_{\check{\alpha}_{\lambda_{p-1}+1}} \cdots \mathcal{T}^{(n_{\lambda_p},m_{\lambda_p})}_{\check{\alpha}_{\lambda_p}} \rangle \\
&\quad \times \prod_{i=1}^{l} t^{(n_i,m_i)}_{\check{\alpha}_i} N^{-2(n_1+m_1+\cdots+n_l+m_l)},
\end{aligned}
\tag{3.33}
$$

where the partitions λ and μ are $\lambda = (1^{n_1+m_1}, 2^{n_2+m_2}, \ldots, p^{n_p+m_p})$ and $\mu = (1^{u_1+v_1}, 2^{u_2+v_2}, \ldots, p^{u_p+v_p})$, $S(\mu) = \binom{\sum_i n_i+m_i}{u_1+v_1}\binom{\sum_i n_i+m_i-(u_1+v_1)}{u_2+v_2}\cdots 1$, $\tilde{S}(\lambda) = (n_1 + m_1)!(n_2 + m_2)! \cdots (n_p + m_p)!$.

Here we have taken $N_1 = N_2 = N_3 = N$ in (3.33), then the correlators can be written as

$$
\begin{aligned}
\langle \mathcal{T}^{(n_1,m_1)}_{\check{\alpha}_1} \cdots \mathcal{T}^{(n_l,m_l)}_{\check{\alpha}_l} \rangle &= N^{2(n_1+m_1)+1+\cdots+2(n_l+m_l)+1} \\
&\quad \cdot \frac{l!c_l}{(n_1 + m_1 + \cdots + n_l + m_l)!\lambda_{\check{\alpha}_1,\ldots,\check{\alpha}_l}} \\
&\quad + \circ (N^{2(n_1+m_1)+1+\cdots+2(n_l+m_l)+1}),
\end{aligned}
\tag{3.34}
$$

where c_l is a constant.

Thus in large N limit, we have

$$
\mathcal{F} \sim \sum_{\check{\alpha}_1 \mid level(\check{\alpha}_1)=n_1+m_1=0}^{\infty} \frac{N}{(n_1 + m_1)!} t^{(n_1,m_1)}_{\check{\alpha}_1}.
\tag{3.35}
$$

For the degrees of Feynman graphs $\omega(\mathcal{G})$ and gauge-invariant operators $\omega(\mathcal{T})$ in the D-colored tensor model, there are the relations as follows [8]:

$$
\begin{aligned}
|F_{\mathcal{G}}| &= \frac{D(D-1)}{2} v + D - \frac{2}{(D-1)!} \omega(\mathcal{G}), \\
|F_{\mathcal{T}}| &= \frac{(D-1)(D-2)}{2} v + D - 1 - \frac{2}{(D-2)!} \omega(\mathcal{T}),
\end{aligned}
\tag{3.36}
$$

where $|F_{\mathcal{G}}|$ and $|F_{\mathcal{T}}|$ denote the number of faces in the Feynman diagrams and the gauge-invariant operators respectively, and $2v$ denotes the number of vertices in the Feynman diagrams.

Then we have the number of faces obtained only by the Wick contractions, i.e.,

$$
|F_{\mathcal{G}}| - |F_{\mathcal{T}}| = 2v + 1 - \omega(\mathcal{G}) + 2\omega(\mathcal{T}),
\tag{3.37}
$$

where we have taken $D = 3$ in $|F_{\mathcal{G}}|$ and $|F_{\mathcal{T}}|$.

From (3.35) and (3.37), there is a relation between the free energy in large N limit and melonic graphs as follows. The highest power of N in each Gaussian average of the gauge-invariant operator is $2v + 1$. It is given by the Feynman diagram with degree zero i.e., melonic graphs. The melonic graphs can be obtained from a elementary melon (see Fig. 15a) with fewer vertices by inserting two vertices connected by 2 edges on one of the edge of the elementary melon which also be called the dressed melon (see Fig. 15b and c).

4 Conclusions

We have given the keystone operators which are the gauge-invariant operators. Then by the keystone operators with addition, multiplication, cut and join operations, we constructed a graded ring with tree and loop operators and enumerated the operators in the graded ring. We have also taken the ring S_2 and S_3 as examples to analyze the kernel and cokernel of the cut-and-join structure in these rings. In terms of the keystones operators, connected tree and loop operators in the ring, we have constructed a two-tensor model with order-3. Moreover we showed that it can be realized by acting on elementary function with exponent of the given operator. By means of the W-representation of this two-tensor model, we have derived the compact expression of correlators and presented the free energy in large N limit.

The Fredkin spin chain exhibits violation of the cluster decomposition property and of the area law for the entanglement entropy, with the presence of anomalous and extremely fast propagation of the excitations after driving the system out-of-equilibrium. It seems that this model extremely promising for applications in quantum information and communication processes. We have established a correspondence between two colored Dyck walks in Fredkin spin chain and tree operators in tensor model. For the number of the length-$2n$ two colored Dyck walks, it is counted by 2^n multiples of the n-th Catalan number. Based on the classification Dyck walks, we gave the number of tree operators with level-l,

Fig. 14 Feynman diagrams contributing to highest power terms of N_1 in $\langle \mathrm{Tr} T^2 \rangle$ and the corresponding length-4 two colored Dyck walks
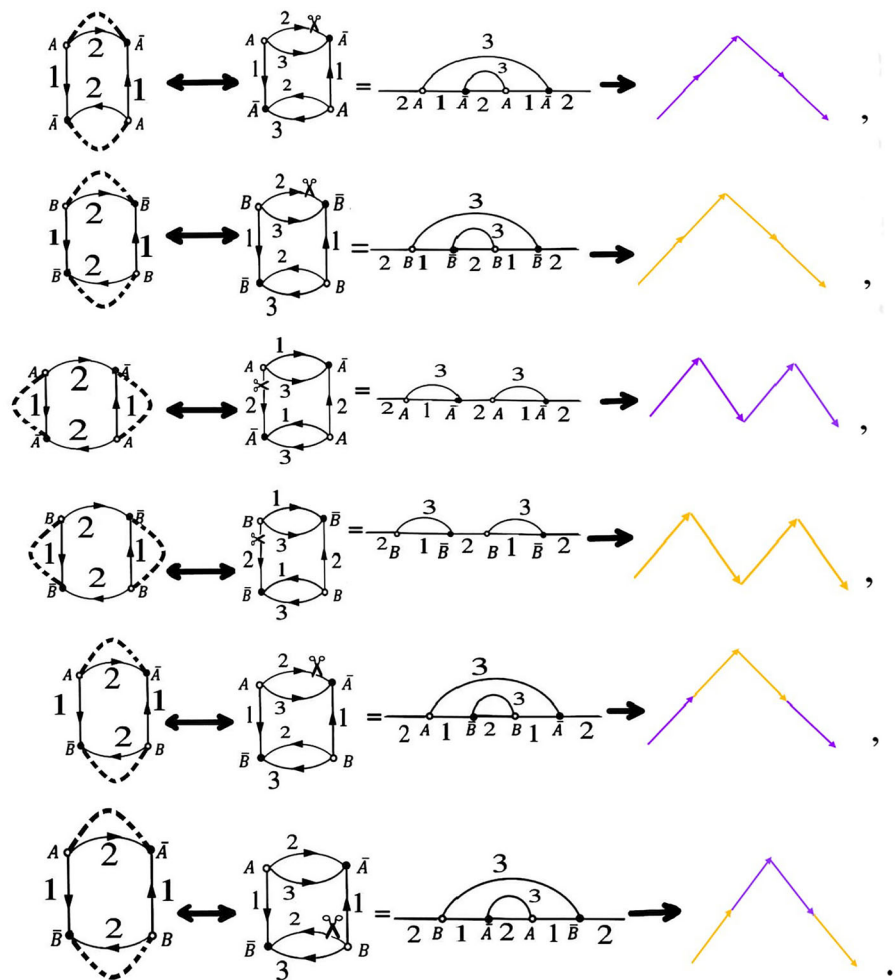
Fig. 15 Examples of melonic graphs
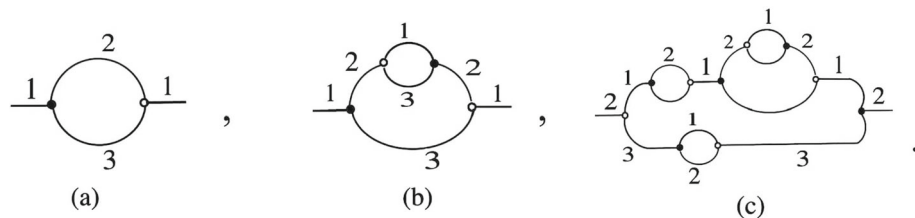
i.e., $\sharp_l^{tree}$. Then the number of connected loop operators can be obtained from the difference between the numbers of connected operators and tree operators. On the other hand, by the collective field computation, we gave the highest power term of N_1 in correlators $\langle \mathrm{Tr} T^n \rangle$ with $N_1 = N_2 N_3$. It was noted that the coefficient C_n of the highest power term of N_1 indeed counts the number of special length-$2n$ colored Dyck walks. For the entanglement entropy of the Fredkin spin chain, it exhibits the entanglement scaling beyond logarithmic scaling in the ordinary critical systems. Quite interestingly, we found that this result can be easily showed from the viewpoint of tensor model. For further research, it would be interesting to explore more properties of the tensor model and Fredkin spin chain via such kind of correspondence.

Appendix A

We list the cut operation Δ acting on the level-3 gauge-invariant operators as follows:

$$\Delta(\mathcal{T}^{(3,0)}_{((23),(12),id)}) = (2N_2 + N_1 N_3)\mathcal{T}^{(2,0)}_{((12),id,id)} + (2N_1 + N_2 N_3)\mathcal{T}^{(2,0)}_{(id,(12),id)}$$
$$+ 2\mathcal{T}^{(2,0)}_{(id,id,(12))} + N_3(\mathcal{T}^{(1,0)}_{(id,id,id)})^2,$$

$$\Delta(\mathcal{T}^{(2,1)}_{((123),id,id)}) = (N_1 + 2N_2 N_3)\mathcal{T}^{(1,1)}_{((12),id,id)} + \mathcal{T}^{(1,0)}_{(id,id,id)}\mathcal{T}^{(0,1)}_{(id,id,id)},$$

$$\Delta(\mathcal{T}^{(2,1)}_{((23),(12),id)}) = (2N_2 + N_1 N_3)\mathcal{T}^{(1,1)}_{((12),id,id)} + N_3\mathcal{T}^{(1,0)}_{(id,id,id)}\mathcal{T}^{(0,1)}_{(id,id,id)},$$

$$\Delta(\mathcal{T}^{(2,1)}_{((123),(23),id)}) = \alpha\mathcal{T}^{(1,1)}_{((12),(12),id)} + N_3\mathcal{T}^{(1,1)}_{((12),id,id)} + \mathcal{T}^{(1,1)}_{(id,(12),id)},$$

$$\Delta(\mathcal{T}^{(2,1)}_{((132),(13),id)}) = (2N_3 + N_1 N_2)\mathcal{T}^{(1,1)}_{((12),(12),id)} + N_2\mathcal{T}^{(1,0)}_{(id,id,id)}\mathcal{T}^{(0,1)}_{(id,id,id)}$$

$$\Delta(\mathcal{T}^{(2,1)}_{((123),(123),id)}) = (2N_2 + N_1 N_3)\mathcal{T}^{(1,0)}_{(id,id,id)}\mathcal{T}^{(0,1)}_{(id,id,id)},$$

$$\Delta(\mathcal{T}^{(2,1)}_{((132),(123),id)}) = N_1\mathcal{T}^{(1,1)}_{((12),id,id)} + N_2\mathcal{T}^{(1,1)}_{(id,(12),id)} + 2N_3\mathcal{T}^{(1,1)}_{((12),(12),id)},$$

$$\Delta(\mathcal{T}^{(2,0)}_{((12),id,id)}\mathcal{T}^{(0,1)}_{(id,id,id)}) = 2\alpha\mathcal{T}^{(1,0)}_{(id,id,id)}\mathcal{T}^{(0,1)}_{(id,id,id)},$$

$$\Delta(\mathcal{T}^{(1,1)}_{((12),id,id)}\mathcal{T}^{(1,0)}_{(id,id,id)}) = (\beta+2)\mathcal{T}^{(1,1)}_{((12),id,id)} + N_2 N_3\mathcal{T}^{(1,0)}_{(id,id,id)}\mathcal{T}^{(0,1)}_{(id,id,id)},$$

$$\Delta(\mathcal{T}^{(1,1)}_{((12),(12),id)}\mathcal{T}^{(1,0)}_{(id,id,id)}) = (\beta+2)\mathcal{T}^{(1,1)}_{((12),(12),id)} + N_3\mathcal{T}^{(1,0)}_{(id,id,id)}\mathcal{T}^{(0,1)}_{(id,id,id)},$$

$$\Delta(\mathcal{T}^{(3,0)}_{((123),id,id)}) = 3\alpha\mathcal{T}^{(2,0)}_{((12),id,id)} + 3(\mathcal{T}^{(1,0)}_{(id,id,id)})^2,$$
$$\Delta(\mathcal{T}^{(3,0)}_{((123),(132),id)}) = 3(N_1\mathcal{T}^{(2,0)}_{((12),id,id)} + N_2\mathcal{T}^{(2,0)}_{(id,(12),id)} + N_3\mathcal{T}^{(2,0)}_{(id,id,(12))}),$$
$$\Delta(\mathcal{T}^{(2,0)}_{((12),id,id)}\mathcal{T}^{(1,0)}_{(id,id,id)}) = (\beta+4)\mathcal{T}^{(2,0)}_{((12),id,id)} + 2\alpha(\mathcal{T}^{(1,0)}_{(id,id,id)})^2,$$
$$\Delta((\mathcal{T}^{(1,0)}_{(id,id,id)})^3) = 3(\beta+2)(\mathcal{T}^{(1,0)}_{(id,id,id)})^2,$$
$$\Delta((\mathcal{T}^{(1,0)}_{(id,id,id)})^2\mathcal{T}^{(0,1)}_{(id,id,id)}) = (2\beta+2)\mathcal{T}^{(1,0)}_{(id,id,id)}\mathcal{T}^{(0,1)}_{(id,id,id)},$$
$$\Delta(\mathcal{T}^{(1,2)}_{((123),id,id)}) = N_2 N_3\mathcal{T}^{(0,2)}_{((12),id,id)},$$
$$\Delta(\mathcal{T}^{(1,2)}_{((23),(12),id)}) = N_3(\mathcal{T}^{(0,1)}_{(id,id,id)})^2,$$
$$\Delta(\mathcal{T}^{(1,2)}_{((123),(23),id)}) = N_3\mathcal{T}^{(0,2)}_{((12),id,id)},$$
$$\Delta(\mathcal{T}^{(1,1)}_{((12),id,id)}\mathcal{T}^{(0,1)}_{(id,id,id)}) = N_2 N_3(\mathcal{T}^{(0,1)}_{(id,id,id)})^2,$$
$$\Delta(\mathcal{T}^{(1,1)}_{((12),(12),id)}\mathcal{T}^{(0,1)}_{(id,id,id)}) = N_3(\mathcal{T}^{(0,1)}_{(id,id,id)})^2,$$
$$\Delta(\mathcal{T}^{(1,0)}_{(id,id,id)}(\mathcal{T}^{(0,1)}_{(id,id,id)})^2) = \beta(\mathcal{T}^{(0,1)}_{(id,id,id)})^2,$$

$$\text{(A.1)}$$

then we may give the kernel

$$\ker^{(3)}(\Delta) = \text{span}\left\{\begin{array}{l}
\end{array}\right.$$

$3(\beta+4)(\beta+2)\mathcal{T}^{(3,0)}_{((23),(12),id)} - 3(\beta+2)((N_1+\alpha)\mathcal{T}^{(2,0)}_{((12),id,id)}\mathcal{T}^{(1,0)}_{(id,id,id)} + (N_2+\tilde\alpha)\mathcal{T}^{(2,0)}_{(id,(12),id)}\mathcal{T}^{(1,0)}_{(id,id,id)}$
$+2\mathcal{T}^{(2,0)}_{(id,id,(12))}\mathcal{T}^{(1,0)}_{(id,id,id)}) + (\beta(12-5N_3) - 4N_1 N_2 + 2(2+N_3{}^2)(N_1+N_2)^2)(\mathcal{T}^{(1,0)}_{(id,id,id)})^3,$

$3(\beta+4)(\beta+2)\mathcal{T}^{(3,0)}_{((23),(123),id)} - 3(\beta+2)((N_3+\hat\alpha)\mathcal{T}^{(2,0)}_{(id,id,(12))}\mathcal{T}^{(1,0)}_{(id,id,id)} + (N_2+\tilde\alpha)\mathcal{T}^{(2,0)}_{(id,(12),id)}\mathcal{T}^{(1,0)}_{(id,id,id)}$
$+2\mathcal{T}^{(2,0)}_{((12),id,id)}\mathcal{T}^{(1,0)}_{(id,id,id)}) + (\beta(12-5N_1) - 4N_3 N_2 + 2(2+N_1{}^2)(N_3+N_2)^2)(\mathcal{T}^{(1,0)}_{(id,id,id)})^3,$

$(\beta+4)(\beta+2)\mathcal{T}^{(3,0)}_{(id,(123),id)} - 3\tilde\alpha(\beta+2)\mathcal{T}^{(2,0)}_{(id,(12),id)}\mathcal{T}^{(1,0)}_{(id,id,id)} + (2\tilde\alpha^2 - \beta - 4)(\mathcal{T}^{(1,0)}_{(id,id,id)})^3,$

$(\beta+4)(\beta+2)\mathcal{T}^{(3,0)}_{((123),(132),id)} - 3(\beta+2)(N_1\mathcal{T}^{(2,0)}_{((12),id,id)}\mathcal{T}^{(1,0)}_{(id,id,id)} + N_2\mathcal{T}^{(2,0)}_{(id,(12),id)}\mathcal{T}^{(1,0)}_{(id,id,id)}$
$+N_3\mathcal{T}^{(2,0)}_{(id,id,(12))}\mathcal{T}^{(1,0)}_{(id,id,id)}) + 2(N_1\alpha + N_2\tilde\alpha + N_3\hat\alpha)(\mathcal{T}^{(1,0)}_{(id,id,id)})^3,$

$\alpha(2N_2 + N_1 N_3)\mathcal{T}^{(2,1)}_{((123),id,id)} - \alpha(N_1 + 2N_2 N_3)\mathcal{T}^{(2,1)}_{((23),(12),id)} - (N_2 - N_2 N_3{}^2)\mathcal{T}^{(2,0)}_{((12),id,id)}\mathcal{T}^{(0,1)}_{(id,id,id)},$

$2\alpha(N_2 + 2N_1 N_3)(N_1 + 2N_2 N_3)[(N_2 + N_1 N_3)\mathcal{T}^{(2,1)}_{((123),(23),id)} - (N_1 + N_2 N_3)\mathcal{T}^{(2,1)}_{((23),(123),id)}]$
$-2\alpha(N_2 + 2N_1 N_3)(N_1 N_3{}^2 - N_1)\mathcal{T}^{(2,1)}_{((123),id,id)} - 2\alpha(N_1 + 2N_2 N_3)(N_2 - N_2 N_3{}^2)\mathcal{T}^{(2,1)}_{(id,(123),id)}$
$-[(N_2 + 2N_1 N_3)(N_1 N_3{}^2 - N_1) - (N_1 + 2N_2 N_3)(N_2 - N_2 N_3{}^2)]\mathcal{T}^{(2,0)}_{((12),id,id)}\mathcal{T}^{(0,1)}_{(id,id,id)},$

$N_3\mathcal{T}^{(1,2)}_{((123),id,id)}, \quad N_2 N_3\mathcal{T}^{(1,2)}_{((23),(23),id)},$

$N_2 N_3\mathcal{T}^{(1,1)}_{((12),(12),id)}\mathcal{T}^{(0,1)}_{(id,id,id)} - N_3\mathcal{T}^{(1,1)}_{(id,id,id)}\mathcal{T}^{(0,1)}_{(id,id,id)},$

$N_1 N_3\mathcal{T}^{(1,0)}_{(id,id,id)}(\mathcal{T}^{(0,1)}_{(id,id,id)})^2 - \beta\mathcal{T}^{(1,1)}_{((12),id,id)}\mathcal{T}^{(0,1)}_{(id,id,id)},$

$(2\beta+2)\mathcal{T}^{(2,0)}_{(id,id,(12))}\mathcal{T}^{(1,0)}_{(id,id,id)} - 2\hat\alpha(\mathcal{T}^{(1,0)}_{(id,id,id)})^2\mathcal{T}^{(0,1)}_{(id,id,id)},$

$\alpha[(N_1 + 2N_2 N_3)\mathcal{T}^{(1,1)}_{((12),id,id)}\mathcal{T}^{(1,0)}_{(id,id,id)} - (\beta+2)\mathcal{T}^{(2,1)}_{((123),id,id)}] - (N_2{}^2 N_3{}^2 - 1)\mathcal{T}^{(2,0)}_{((12),id,id)}\mathcal{T}^{(0,1)}_{(id,id,id)},$

$2\alpha(N_1 + 2N_2 N_3)(N_2 + 2N_1 N_3)[(N_1 + N_2 N_3)\mathcal{T}^{(1,1)}_{((12),id,id)}\mathcal{T}^{(1,0)}_{(id,id,id)} - (\beta+2)\mathcal{T}^{(2,1)}_{((123),(23),id)}]$
$+2\alpha(N_2 - N_1 N_3)N_3(\beta+2)\mathcal{T}^{(2,1)}_{((123),id,id)} + 2\alpha(N_1 + 2N_2 N_3)(\beta+2)\mathcal{T}^{(2,1)}_{(id,(123),id)}$
$-(N_1 + 3N_2 N_3 + 2N_1 N_3{}^2)(\beta+2)\mathcal{T}^{(2,0)}_{((12),id,id)}\mathcal{T}^{(0,1)}_{(id,id,id)},$

$(2\beta+2)[(2N_3 + N_1 N_2)\mathcal{T}^{(1,1)}_{(id,(12),id)}\mathcal{T}^{(1,0)}_{(id,id,id)} - (\beta+2)\mathcal{T}^{(2,1)}_{((13),(132),id)}]$
$-(2N_1 N_3{}^2 - 2N_1)(\mathcal{T}^{(1,0)}_{(id,id,id)})^2\mathcal{T}^{(0,1)}_{(id,id,id)},$

$3(\beta+4)(\beta+2)\mathcal{T}^{(3,0)}_{((123),(23),id)} - 3(\beta+2)((N_1+\alpha)\mathcal{T}^{(2,0)}_{(id,id,id)}\mathcal{T}^{(1,0)}_{(id,id,id)} + (N_3+\hat\alpha)\mathcal{T}^{(2,0)}_{(id,id,(12))}\mathcal{T}^{(1,0)}_{(id,id,id)}$
$+2\mathcal{T}^{(2,0)}_{(id,(12),id)}\mathcal{T}^{(1,0)}_{(id,id,id)}) + (\beta(12-5N_2) - 4N_1 N_3 + 2(2+N_2{}^2)(N_1+N_3)^2)(\mathcal{T}^{(1,0)}_{(id,id,id)})^3,$

$(\beta+4)(\beta+2)\mathcal{T}^{(3,0)}_{((123),id,id)} - 3\alpha(\beta+2)\mathcal{T}^{(2,0)}_{((12),id,id)}\mathcal{T}^{(1,0)}_{(id,id,id)} + (2\alpha^2 - \beta - 4)(\mathcal{T}^{(1,0)}_{(id,id,id)})^3,$

$(\beta+4)(\beta+2)\mathcal{T}^{(3,0)}_{(id,id,(123))} - 3\hat\alpha(\beta+2)\mathcal{T}^{(2,0)}_{(id,id,(12))}\mathcal{T}^{(1,0)}_{(id,id,id)} + (2\hat\alpha^2 - \beta - 4)(\mathcal{T}^{(1,0)}_{(id,id,id)})^3,$

$(\beta+2)\mathcal{T}^{(2,1)}_{((132),(123),id)} - N_1\mathcal{T}^{(1,1)}_{((12),id,id)}\mathcal{T}^{(1,0)}_{(id,id,id)} - N_2\mathcal{T}^{(1,1)}_{(id,(12),id)}\mathcal{T}^{(1,0)}_{(id,id,id)}$
$-2N_3\mathcal{T}^{(1,1)}_{((12),(12),id)}\mathcal{T}^{(1,0)}_{(id,id,id)} + (\mathcal{T}^{(1,0)}_{(id,id,id)})^2\mathcal{T}^{(0,1)}_{(id,id,id)},$

$\tilde\alpha(2N_1 + N_2 N_3)\mathcal{T}^{(2,1)}_{(id,(123),id)} - \tilde\alpha(N_2 + 2N_1 N_3)\mathcal{T}^{(2,1)}_{((12),(23),id)} - (N_1 - N_1 N_3{}^2)\mathcal{T}^{(2,0)}_{(id,(12),id)}\mathcal{T}^{(0,1)}_{(id,id,id)},$

$2\tilde\alpha(N_2 + 2N_1 N_3)(N_1 + 2N_2 N_3)[(N_2 + N_1 N_3)\mathcal{T}^{(2,1)}_{((123),(23),id)} - (N_1 + N_2 N_3)\mathcal{T}^{(2,1)}_{((23),(123),id)}]$
$-2\tilde\alpha(N_2 + 2N_1 N_3)(N_1 N_3{}^2 - N_1)\mathcal{T}^{(2,1)}_{((123),id,id)} - 2\tilde\alpha(N_1 + 2N_2 N_3)(N_2 - N_2 N_3{}^2)\mathcal{T}^{(2,1)}_{(id,(123),id)}$
$-[(N_2 + 2N_1 N_3)(N_1 N_3{}^2 - N_1) - (N_1 + 2N_2 N_3)(N_2 - N_2 N_3{}^2)]\mathcal{T}^{(2,0)}_{(id,(12),id)}\mathcal{T}^{(0,1)}_{(id,id,id)},$

$N_3\mathcal{T}^{(1,2)}_{(id,(123),id)} - N_1 N_3\mathcal{T}^{(1,2)}_{((23),(123),id)}, \quad \mathcal{T}^{(1,1)}_{((12),(12),id)}\mathcal{T}^{(0,1)}_{(id,id,id)} - \mathcal{T}^{(1,2)}_{((23),(12),id)}, \quad \beta\mathcal{T}^{(1,1)}_{((12),(12),id)}\mathcal{T}^{(0,1)}_{(id,id,id)} - N_3\mathcal{T}^{(1,0)}_{(id,id,id)}(\mathcal{T}^{(0,1)}_{(id,id,id)})^2,$

$N_1\mathcal{T}^{(1,1)}_{((12),(12),id)}\mathcal{T}^{(0,1)}_{(id,id,id)} - N_3\mathcal{T}^{(1,1)}_{(id,(12),id)}\mathcal{T}^{(0,1)}_{(id,id,id)}, \quad N_2 N_3\mathcal{T}^{(1,0)}_{(id,id,id)}(\mathcal{T}^{(0,1)}_{(id,id,id)})^2 - \beta\mathcal{T}^{(1,1)}_{((12),id,id)}\mathcal{T}^{(0,1)}_{(id,id,id)},$

$(2\beta+2)\mathcal{T}^{(2,0)}_{((12),id,id)}\mathcal{T}^{(0,1)}_{(id,id,id)} - 2\alpha(\mathcal{T}^{(1,0)}_{(id,id,id)})^2\mathcal{T}^{(0,1)}_{(id,id,id)},$

$(2\beta+2)\mathcal{T}^{(2,0)}_{(id,(12),id)}\mathcal{T}^{(0,1)}_{(id,id,id)} - 2\tilde\alpha(\mathcal{T}^{(1,0)}_{(id,id,id)})^2\mathcal{T}^{(0,1)}_{(id,id,id)},$

$\tilde\alpha[(N_2 + 2N_1 N_3)\mathcal{T}^{(1,1)}_{(id,(12),id)}\mathcal{T}^{(1,0)}_{(id,id,id)} - (\beta+2)\mathcal{T}^{(2,1)}_{(id,(123),id)}] - (N_2{}^2 N_3{}^2 - 1)\mathcal{T}^{(2,0)}_{(id,(12),id)}\mathcal{T}^{(0,1)}_{(id,id,id)},$

$(2\beta+2)[(2N_3 + N_1 N_2)\mathcal{T}^{(1,1)}_{((12),id,id)}\mathcal{T}^{(1,0)}_{(id,id,id)} - (\beta+2)\mathcal{T}^{(2,1)}_{((132),(13),id)}]$
$-(2N_2 N_3{}^2 - 2N_2)(\mathcal{T}^{(1,0)}_{(id,id,id)})^2\mathcal{T}^{(0,1)}_{(id,id,id)},$

$(2\beta+2)[(2N_3 + N_1 N_2)\mathcal{T}^{(1,1)}_{((12),(12),id)}\mathcal{T}^{(1,0)}_{(id,id,id)} - (\beta+2)\mathcal{T}^{(2,1)}_{((123),(123),id)}]$
$-(2N_3{}^2 - 2)(\mathcal{T}^{(1,0)}_{(id,id,id)})^2\mathcal{T}^{(0,1)}_{(id,id,id)}$

$$\text{(A.2)}$$

References

1. P. Di Francesco, P. Ginsparg, J. Zinn-Justin, 2D gravity and random matrices. Phys. Rep. **254**, 133 (1995)

2. J. Ambjørn, B. Durhuus, T. Jonsson, Three-dimensional simplicial quantum gravity and generalized matrix models. Mod. Phys. Lett. A **6**, 1133 (1991)

3. M. Gross, Tensor models and simplicial quantum gravity in $>2-D$. Nucl. Phys. Proc. Suppl. **25 A**, 144 (1992)

4. N. Sasakura, Tensor model for gravity and orientability of manifold. Mod. Phys. Lett. A **6**, 2613 (1991)

5. R. Gurau, The $1/N$ expansion of colored tensor models. Ann. Henri Poincaré **12**, 829 (2011). arXiv:1011.2726 [gr-qc]

6. R. Gurau, V. Rivasseau, The $1/N$ expansion of colored tensor models in arbitrary dimension. Europhys. Lett. **95**, 50004 (2011). arXiv:1101.4182 [gr-qc]

7. R. Gurau, The complete $1/N$ expansion of colored tensor models in arbitrary dimension. Ann. Henri Poincaré **13**, 399 (2012). arXiv:1102.5759 [gr-qc]

8. R. Gurau, J.P. Ryan, Colored tensor models—a review. SIGMA **8**, 020 (2012). arXiv:1109.4812

9. V. Bonzom, R. Gurau, A. Riello, V. Rivasseau, Critical behavior of colored tensor models in the large N limit. Nucl. Phys. B **853**, 174 (2011). arXiv:1105.3122

10. R. Gurau, *Random Tensors* (Oxford University Press, Oxford, 2016)

11. D. Benedetti, J. Ben Geloun, D. Oriti, Functional renormalisation group approach for tensorial group field theory: a rank-3 model. JHEP **1503**, 084 (2015). arXiv:1411.3180

12. V. Lahoche, D. Oriti, V. Rivasseau, Renormalization of an abelian tensor group field theory: solution at leading order. JHEP **1504**, 095 (2015). arXiv:1501.02086

13. R.C. Avohou, V. Rivasseau, A. Tanasa, Renormalization and Hopf algebraic structure of the 5-dimensional quartic tensor field theory. J. Phys. A: Math. Theor. **48**, 485204 (2015). arXiv:1507.03548 [math-ph]

14. D. Benedetti, V. Lahoche, Functional renormalization group approach for tensorial group field theory: a rank-6 model with closure constraint. Class. Quantum Gravity **33**, 095003 (2016). arXiv:1508.06384

15. J. Ben Geloun, Two and four-loop β-functions of rank 4 renormalizable tensor field theories. Class. Quantum Gravity **29**, 235011 (2012). arXiv:1205.5513

16. J. Ben Geloun, D.O. Samary, $3D$ tensor field theory: renormalization and one-loop β-functions. Ann. Henri Poincaré **14**, 1599 (2013). arXiv:1201.0176

17. V. Rivasseau, Why are tensor field theories asymptotically free? Europhys. Lett. **111**, 60011 (2015). arXiv:1507.04190

18. R. Gurau, The $1/N$ expansion of tensor models with two symmetric tensors. Commun. Math. Phys. **360**, 985 (2018). arXiv:1706.05328

19. D. Benedetti, S. Carrozza, R. Gurau, M. Kolanowski, The $1/N$ expansion of the symmetric traceless and the antisymmetric tensor models in rank three. Commun. Math. Phys. **371**, 55 (2019). arXiv:1712.00249

20. J. Ben Geloun, S. Ramgoolam, Counting tensor model observables and branched covers of the 2-sphere. Ann. Inst. Henri Poincaré Comb. Phys. Interact. **1**, 77 (2014). arXiv:1307.6490

21. J. Ben Geloun, S. Ramgoolam, Tensor models, Kronecker coefficients and permutation centralizer Algebras. JHEP **11**, 092 (2017). arXiv:1708.03524

22. R. de Mello Koch, D. Gossman, L. Tribelhorn, Gauge invariants, correlators and holography in bosonic and fermionic tensor models. JHEP **09**, 011 (2017). arXiv:1707.01455

23. R. de Mello Koch, D. Gossman, N. Tahiridimbisoa, A. Mahu, Holography for tensor models. Phys. Rev. D **101**, 046004 (2020). arXiv:1910.13982

24. H. Itoyama, A. Mironov, A. Morozov, Ward identities and combinatorics of rainbow tensor models. JHEP **06**, 115 (2017). arXiv:1704.08648

25. H. Itoyama, A. Mironov, A. Morozov, Rainbow tensor model with enhanced symmetry and extreme melonic dominance. Phys. Lett. B **771**, 180 (2017). arXiv:1703.04983

26. H. Itoyama, A. Mironov, A. Morozov, Cut and join operator ring in tensor models. Nucl. Phys. B **932**, 52 (2018). arXiv:1710.10027

27. H. Itoyama, A. Mironov, A. Morozov, Tensorial generalization of characters. JHEP **12**, 127 (2019). arXiv:1909.06921

28. A. Morozov, Sh. Shakirov, Generation of matrix models by $\hat{W}$-operators. JHEP **04**, 064 (2009). arXiv:0902.2627

29. R. Wang, C.H. Zhang, F.H. Zhang, W.Z. Zhao, CFT approach to constraint operators for (β-deformed) Hermitian one-matrix models. Nucl. Phys. B **985**, 115989 (2022). arXiv:2203.14578

30. V. Mishnyakov, A. Oreshina, Superintegrability in β-deformed Gaussian Hermitian matrix model from W-operators. Eur. Phys. J. C **82**, 548 (2022). arXiv:2203.15675

31. R. Wang, F. Liu, C.H. Zhang, W.Z. Zhao, Superintegrability for (β-deformed) partition function hierarchies with W-representations. Eur. Phys. J. C **82**, 902 (2022). arXiv:2206.13038

32. A. Bawane, P. Karimi, P. Sułkowski, Proving superintegrability in β-deformed eigenvalue models. SciPost Phys. **13**, 069 (2022). arXiv:2206.14763

33. A. Alexandrov, On W-operators and superintegrability for dessins d'enfant. Eur. Phys. J. C **83**, 147 (2023). arXiv:2212.10952

34. A. Mironov, V. Mishnyakov, A. Morozov, A. Popolitov, R. Wang, W.Z. Zhao, Interpolating matrix models for WLZZ series. Eur. Phys. J. C **83**, 377 (2023). arXiv:2301.04107

35. H. Itoyama, A. Mironov, A. Morozov, Complete solution to Gaussian tensor model and its integrable properties. Phys. Lett. B **802**, 135237 (2020). arXiv:1910.03261

36. B. Kang, L.Y. Wang, K. Wu, J. Yang, W.Z. Zhao, W-representation of rainbow tensor model. JHEP **05**, 228 (2021). arXiv:2104.01332

37. L.Y. Wang, R. Wang, K. Wu, W.Z. Zhao, W-representations of the fermionic matrix and Aristotelian tensor models. Nucl. Phys. B **973**, 115612 (2021). arXiv:2110.14269

38. V. Bonzom, R. Gurau, V. Rivasseau, Random tensor models in the large N limit: uncoloring the colored tensor models. Phys. Rev. D **85**, 084037 (2012). arXiv:1202.3637 [hep-th]

39. L. Dell'Anna, O. Salberger, L. Barbiero, A. Trombettoni, V.E. Korepin, Violation of cluster decomposition and absence of light-cones in local integer and half-integer spin chains. Phys. Rev. B **94**, 155140 (2016). arXiv:1604.08281 [cond-mat.str-el]

40. O. Salberger, V. Korepin, Entangled spin chain. Rev. Math. Phys. **29**, 1750031 (2017)

41. F. Sugino, Highly entangled spin chains and $2D$ quantum gravity. Symmetry **12**, 916 (2020). arXiv:2005.00257